ISSN 2096-7071 (Print)
ISSN 2096-3101 (Online)
CN 10-1629/R1

CHINA CDC WEEKLY

Vol. 7 No. 32 Aug. 8, 2025

中国疾病预防控制中心周报

National Fitness Day

August 8, 2025

ISSN 2096-7071

Cover Image: adapted from General Administration of Sport of China, https://www.sport.gov.cn/qts/n4986/c23457225/-content.html.

Commentary

National Fitness Day: Evolving from "Getting Active" to "Promoting Health"

Qiang Feng[1,#]

Physical activity represents a fundamental pillar of healthy living and serves as a critical determinant of population health outcomes. The World Health Organization (WHO) identifies physical inactivity as the fourth leading risk factor for global mortality, accounting for approximately 3.2 million deaths annually (*1*). Recognizing this significant public health challenge, nations worldwide have implemented comprehensive strategies to promote physical fitness among their populations. China formally established "National Fitness Day" in 2009, designating August 8 as an annual nationwide initiative dedicated to encouraging physical activity participation. This landmark decision not only commemorates the legacy of the 2008 Beijing Olympics but also signifies a strategic shift from prioritizing elite athletic performance toward fostering widespread community engagement in sports and fitness activities.

National Fitness Day serves as a pivotal mechanism for promoting public health on a national scale, utilizing diverse promotional slogans each year to stimulate community engagement in physical activity. The inaugural campaign in 2009 featured inspiring themes such as "Daily Exercise, Daily Joy," "Strong Body, Better Life," and "Fitness for All, Together We Move." In subsequent years, these slogans evolved to reflect changing national priorities, including "One Hour of Daily Exercise for a Lifetime of Health" (2012) and "Advancing National Fitness for a Moderately Prosperous Society" (2020), demonstrating the progressive integration of physical fitness into broader national health objectives.

In recent years, the thematic focus of National Fitness Day has become increasingly sophisticated and multifaceted, strategically aligning with national priorities and major sporting events. For instance, the 2023 theme, "National Fitness Paints a Happier Life," capitalized on the widespread enthusiasm generated by the Beijing Winter Olympics, thereby amplifying the cultural and societal significance of fitness initiatives across the nation. The 2024 campaign, themed "Fitness for All, Celebrating the Olympics," strategically coincided with the Paris Olympics and successfully mobilized over 20,000 events nationwide, engaging more than 10 million participants — a testament to the initiative's remarkable societal impact and organizational effectiveness. In 2025, the 17th National Fitness Day adopted the dynamic slogan "Get Moving for Fitness," with the National Olympic Sports Center leading coordination efforts alongside seven provincial hubs to establish a comprehensive online-offline event framework (*2*). This evolution represents a fundamental transformation: National Fitness Day activities have progressed from initial single-themed promotional events to a sophisticated, coordinated national movement that encourages sustained engagement in fitness and health initiatives throughout the year. This strategic development has positioned National Fitness Day as a pivotal mechanism for advancing the "Healthy China" strategy at the grassroots level, creating lasting behavioral change rather than merely temporary awareness.

Over the past decade, China has achieved remarkable progress in its national fitness initiative across policy development, infrastructure expansion, and public participation. The national fitness program gained formal recognition as a national strategy in 2014 (*3*). Subsequently, the "Healthy China 2030" Plan Outline, launched in 2016 (*4*), established this initiative as a fundamental pillar of the national health policy framework. The revised Sports Law, enacted in 2022, legally codified "National Fitness Day" as an official observance and strengthened governmental obligations to advance this initiative (*5*). Infrastructure developments have been equally impressive: by 2024, China's sports facilities reached 4.84 million, with per capita sports area expanding from 1.46 m^2 in 2013 to 3.0 m^2 (*6*). The "15-Minute Fitness Circle"initiative has enhanced accessibility, while the availability of free or low-cost public sports venues has consistently expanded (*7*). Regular physical activity participation among Chinese citizens rose from 28.2% in 2007 (*8*) to 37.2% in 2020 (*9*). Furthermore, the national physical fitness qualification rate has shown consistent

improvement, reaching 90.4% (*10*). Simultaneously, scientific research into exercise health benefits has intensified. The development of innovative service platforms, including exercise-for-health centers and sports-health integration facilities, has provided crucial scientific support and established new pathways for advancing the national fitness strategy.

Despite these substantial achievements, significant challenges persist that require targeted intervention. Regional disparities in infrastructure development and program accessibility continue to create unequal opportunities for physical activity participation across different geographic areas. Furthermore, certain demographic groups — particularly sedentary populations, individuals with chronic conditions, and those in underserved communities — remain inadequately engaged in national fitness initiatives. The absence of comprehensive scientific guidance and personalized exercise prescription represents another critical gap that limits the effectiveness of current programs.

doi: 10.46234/ccdcw2025.176

[#] Corresponding author: Qiang Feng, fengqiang@ciss.cn.

[1] National Fitness and Scientific Exercise Center, China Institute of Sport Science, Beijing, China.

Submitted: July 23, 2025
Accepted: August 04, 2025
Issued: August 08, 2025

REFERENCES

1. World Health Organization. WHO guidelines on physical activity and sedentary behaviour. Geneva: WHO. 2020. https://www.who.int/publications/i/item/9789240015128.
2. General Administration of Sport of China. Office of the general administration notice on organizing the 2025 national fitness day themed activities. 2025. https://www.sport.gov.cn/gdnps/content.jsp?id=28565226. [2025-7-11]. (In Chinese).
3. State Council of the People's Republic of China. Opinions on accelerating the development of sports industry and promoting sports consumption. 2014. https://www.gov.cn/zhengce/content/2014-10/20/content_9152.htm. [2025-7-11]. (In Chinese).
4. Central Committee of the Communist Party of China, State Council of the People's Republic of China. Outline of the healthy China 2030 plan. 2016. https://www.gov.cn/gongbao/content/2016/content_5133024.htm. [2025-7-11]. (In Chinese).
5. People's Republic of China. Sports law of the People's Republic of China (The standing committee of the Thirteenth national people's congress of the People's Republic of China revised on June 24, 2022). 2022. https://www.gov.cn/xinwen/2022-06/25/content_5697693.htm. [2025-7-11]. (In Chinese).
6. General Administration of Sport of China. 20-year data trends in China's sports venue development: a national statistical survey comparison. 2025. https://www.sport.gov.cn/n20001280/n20745751/c28556256/content.html. [2025-7-11]. (In Chinese).
7. General Administration of Sport of China. Office of the General Administration issues "Notice"to further strengthen management of free or low-cost open access to public sports venues. 2024. https://www.sport.gov.cn/n20001280/n20745751/c28336843/content.html. [2025-7-11]. (In Chinese).
8. General Administration of Sport of China. Bulletin on the status of physical exercise among urban and rural residents in China 2007. 2008. https://www.sport.gov.cn/qts/n4986/c670088/content.html. [2025-7-11]. (In Chinese).
9. General Administration of Sport of China. Bulletin on the status of national fitness activities 2020. 2022. https://www.sport.gov.cn/n315/n329/c24335053/content.html. [2025-7-11]. (In Chinese).
10. China Physical Fitness Surveillance Center. Bulletin on the fifth national physical fitness surveillance. 2021. https://www.ciss.cn/zhxw/info/2021/32028.html. [2025-7-22]. (In Chinese).

Qiang Feng
Associate Professor, China Institute of Sport Science
Deputy Director, National Physical Fitness and Scientific Exercise Center, China Institute of Sport Science

Vital Surveillances

Epidemiological Characteristics and Influencing Factors of Bacillary Dysentery Outbreaks — China, 2008–2024

Ao Luo[1,2]; Yang Song[3]; Fengfeng Liu[3]; Zhaorui Chang[3,#]; Yanping Zhang[3]

ABSTRACT

Introduction: The incidence of bacillary dysentery (BD) has declined significantly in China, yet BD outbreaks persist across multiple regions. This study describes the epidemiological characteristics of BD outbreaks nationwide and proposes targeted interventions for outbreak prevention and control.

Methods: This study obtained BD outbreak data from the Public Health Emergency Event Surveillance System in China for descriptive epidemiological analysis and employed unconditional logistic regression to identify factors influencing outbreak magnitude.

Results: During 2008–2024, China reported 176 BD outbreaks involving 9,854 cases and four deaths. The median attack rate and interquartile range for outbreaks were 5.99% (2.53%, 13.32%). Annual outbreak reports decreased throughout the study period, with no outbreaks documented in 2023 and 2024. Among all outbreaks, 75.6% occurred in rural areas, and 76.7% were reported in schools. Most outbreaks occurred during September or October (52.3%). *Shigella sonnei* and *Shigella flexneri* were the predominant outbreak pathogens; the principal transmission routes were waterborne (47.7%) and foodborne (23.9%). Median and interquartile ranges for response times and case counts were 3 (2, 6) days and 44 (25, 71) cases, respectively. Factors associated with larger outbreak size included *S. sonnei* as the causative pathogen, waterborne transmission, and outbreak duration of eight days or longer.

Conclusions: In China, BD outbreak frequency has decreased substantially. September and October represent high-risk months, with schools serving as the primary outbreak setting during the back-to-school season. Strengthening BD prevention and control in educational institutions, with particular attention to water and food hygiene, remains essential for outbreak prevention.

Bacillary dysentery (BD) represents an intestinal infectious disease caused by *Shigella* infection, characterized by diarrhea, fever, and abdominal pain, with potential blood or mucus in stools (*1*). The World Health Organization estimates that BD affects over 270 million individuals annually, accounting for 5%–15% of diarrheal diseases worldwide and representing the second leading cause of diarrheal death across all age groups (*2*). In China, BD is classified as a Class B notifiable communicable disease. Through sustained economic development and proactive public health interventions, marked reductions in both incidence and mortality have been achieved during the past three decades. The incidence rate declined by 93.2% from 35.4 per 100,000 in 2005 to 2.4 per 100,000 in 2024 (*3*). Despite these achievements, BD outbreaks continue to occur across many regions of China, with frequent reports of cases in collective settings such as schools (*4*–*5*). Identifying the sources of infection and determining the contributing factors remains crucial for preventing and controlling these outbreaks. This study analyzes nationwide data on BD outbreaks from 2008 to 2024, aiming to explore occurrence patterns and epidemiological characteristics, define high-risk outbreak scenarios, and generate evidence-based recommendations for enhancing outbreak response strategies.

METHODS

This study extracted BD outbreak data from reports in the China Public Health Emergency Surveillance System, covering January 1, 2008, through December 31, 2024. All reported outbreaks were identified following the *Handbook for Prevention and Treatment of Bacillary Dysentery* and verified by the responsible county-level CDC, which conducted comprehensive investigations and implemented response measures for confirmed BD outbreaks.

This study extracted epidemiological variables from investigation reports of each outbreak to establish its

database. These variables included reporting province, onset dates of index and terminal cases, outbreak setting, transmission route, case counts, exposed population size, reporting date, outbreak closure date, and etiological confirmation results.

This study then described seasonal patterns using a seasonal index, calculated by dividing the average monthly outbreaks by the overall monthly average during the study period. A seasonal index exceeding 1.0 indicates a significant seasonal pattern. It defined outbreak duration as the interval between the first case' s and last case's onset dates. Response time was defined as the interval between the first case's onset and the reporting date. This study calculated the attack rate as the number of cases divided by the number of individuals exposed.

Next, this study used frequencies and proportions to describe categorical variables and medians with interquartile ranges (IQR) to characterize numerical variables. The Mann-Kendall trend test assessed trends in case numbers, outbreak size, and duration. This study employed unconditional logistic regression to identify factors associated with outbreak size. Variables with $P<0.1$ in univariate analysis were included in multivariate analysis, followed by bidirectional stepwise regression (entry $P<0.10$, removal $P>0.05$). Statistical analyses were performed using R (version 4.3.3, R Foundation, Vienna, Austria), with two-sided $P<0.05$ considered statistically significant.

RESULTS

Between 2008 and 2024, China reported 176 BD outbreaks comprising 9,854 cases and 4 deaths. The annual number of reported outbreaks demonstrated a fluctuating downward trend with strong negative correlation to year (r_s=–0.88, $P<0.001$). The distribution across time periods showed 53% of BD outbreaks occurred during 2008–2012, 33% during 2013–2017, and 14% during 2018–2022, with no outbreaks reported in 2023 or 2024. The median attack rate was 5.99% (interquartile range: 2.53%, 13.32%) (Figure 1).

Outbreaks were documented across 102 cities in 22 provincial-level administrative divisions (PLADs). The 5 PLADs with the highest outbreak frequencies were Hunan (46), Guangxi (22), Chongqing (12), Sichuan (12), and Guizhou (11), all situated in southwestern China. While outbreaks occurred throughout the year, 52.3% were concentrated in September and October, with seasonal indices of 4.2 and 2.0 for these months, respectively (Figure 2).

Rural areas accounted for 75.6% of outbreaks (133/176), predominantly occurring in schools (72.2%, 96/133) and villages (24.8%, 33/133). Urban outbreaks represented 24.4% (43/176) of cases, with schools being the most frequent setting (90.7%, 39/43), followed by mental hospitals (4 outbreaks), construction sites (3 outbreaks), and restaurants (1 outbreak). Reporting timeliness differed significantly across settings (H=24.5, $P<0.001$), with school outbreaks reported within a median of 3 (2,5) days compared to village outbreaks at 7 (4,11) days (Table 1).

Waterborne transmission predominated, accounting for 47.7% (84/176) of outbreaks. Among waterborne

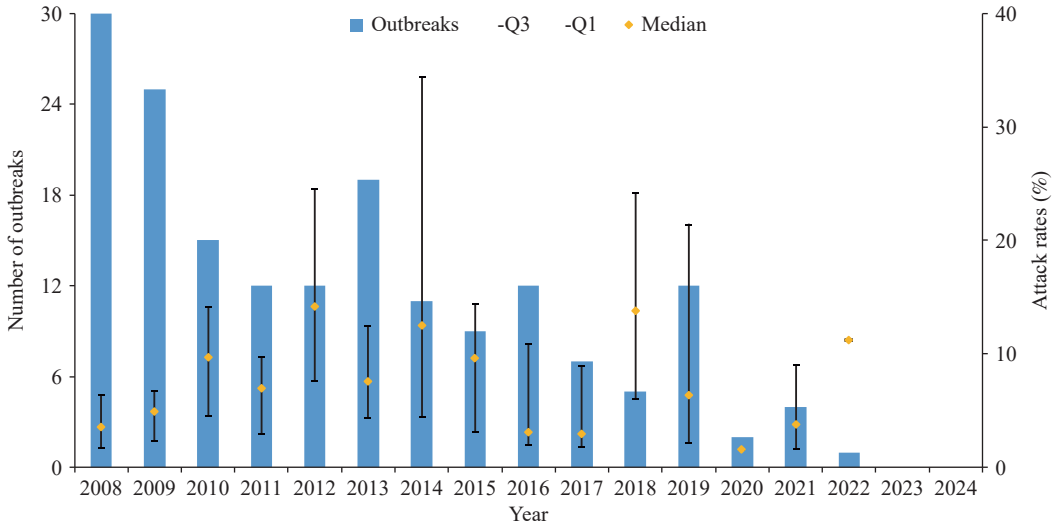

FIGURE 1. Annual number of bacillary dysentery outbreaks and corresponding attack rates in China, 2008–2024.

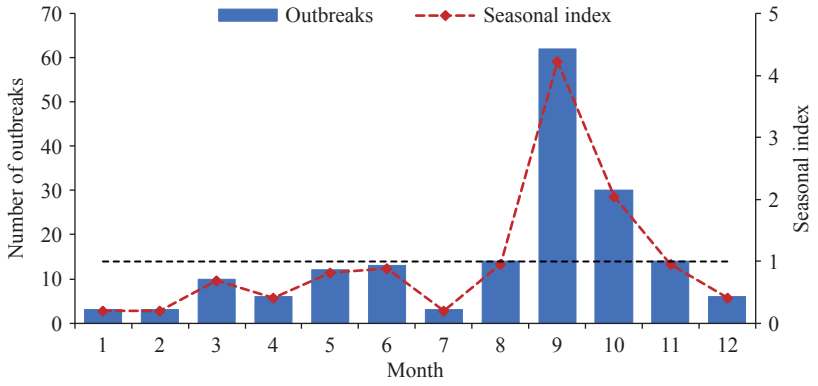

FIGURE 2. Temporal distribution of bacillary dysentery outbreaks in China, 2008–2024.

cases, 63 outbreaks (75%) involved drinking water samples exceeding microbial safety standards, while *Shigella* was successfully isolated from water samples in 34 outbreaks (40.5%). School and village waterborne outbreaks comprised 47.4% and 54.5% of their respective totals. In educational settings, contamination sources included self-supplied well water (73%), secondary water supply systems (8%), water storage tanks (6%), and cafeteria reserve water (6%). Village waterborne outbreaks resulted from contaminated river and spring water exposure through daily activities and vegetable washing during rural gatherings. Foodborne transmission ranked second at 23.9% of outbreaks. The 34 school-based foodborne outbreaks primarily stemmed from contaminated, undercooked, or raw food consumption and poor dietary hygiene. Food handlers or nursery staff were identified as *Shigella* carriers in 15 outbreaks, while *Shigella* was detected in stored food samples from 6 outbreaks. Village foodborne outbreaks occurred through consumption of meals at patients' homes and food preparation using contaminated water.

Laboratory confirmation was achieved in 87.5% (154/176) of BD outbreaks. Among the 119 outbreaks with identified pathogen types, *S. sonnei* (69.7%) was the most frequently detected organism, followed by *S. flexneri* (27.7%). One *S. boydii* infection and two mixed infections were also documented.

Using the median number of outbreak cases reported as a cut-off, outbreaks were categorized into large size (cases ≥44) and small size (cases <44) groups for factor analysis. Univariate analysis found that occurrence site, transmission route, response time, duration, and pathogen were associated with outbreak size (P<0.1). Multivariate unconditional logistic regression found that waterborne transmission [adjusted odds ratios (a*OR*)=5.4, 95% confidence interval (*CI*): 1.9–15.3], *S. sonnei* infection (a*OR*=4.3, 95% *CI*: 1.7–10.9), and outbreak duration (compared with ≤3 days, a*OR* for ≥8 days =3.8, 95% *CI*: 1.0–13.8) were associated with a higher risk of large size outbreaks (Table 2).

DISCUSSION

This study demonstrates a significant decline in BD outbreaks across China during 2008–2024, consistent with the downward trend in BD cases reported through the national notifiable communicable disease surveillance system (*3*). This substantial reduction can be attributed to comprehensive nationwide prevention and control measures, including the expansion of centralized water supply systems, enhanced water quality monitoring protocols, implementation of fecal waste treatment and sanitation improvement programs, and increased public hygiene awareness (*6*). The marked decline observed after 2020 may be associated with non-pharmaceutical interventions implemented during the coronavirus disease 2019 (COVID-19) pandemic, which likely reduced intestinal disease transmission by limiting interpersonal contact and environmental exposure (*7*).

BD outbreaks were predominantly concentrated in southwestern PLADs. Previous research has identified undulating terrain, favorable climatic conditions, and limited economic development as key risk factors in southwestern China (*8*). The challenging topography restricts regional economic growth, thereby limiting infrastructure development for safe water supply systems and waste treatment facilities. This results in poor sanitation conditions that facilitate *Shigella* transmission. Additionally, the temperature and humidity conditions characteristic of southwestern regions create favorable environments for bacterial

TABLE 1. Transmission routes, pathogens, and reporting timeliness of bacillary dysentery outbreaks in different settings in China, 2008–2024.

Outbreak sites	Outbreaks, *n* (%)	Route of transmission, *n* (%)				Pathogen, *n* (%)					Reported time, day *M* (Q_1–Q_3)
		Waterborne	Foodborne	Contact-borne	Unknown	*Shigella sonnei*	*Shigella flexneri*	*Shigella boydii*	Mixed infection	Total	
School	135 (76.7)	64 (47.4)	34 (25.2)	6 (4.4)	31 (23.0)	79 (79.0)	19 (19.0)	1 (1.0)	1 (1.0)*	100 (100.0)	3 (2–5)
Village	33 (18.8)	18 (54.5)	6 (18.2)	1 (3.0)	8 (24.2)	4 (25.0)	12 (75.0)	0 (0.0)	0 (0.0)	16 (100.0)	7 (4–11)
Hospital	4 (2.3)	1 (25.0)	0 (0.0)	3 (75.0)	0 (0.0)	0 (0.00)	1 (100.0)	0 (0.0)	0 (0.0)	1 (100.0)	16 (8–23)
Building site	3 (1.7)	1 (33.3)	1 (33.3)	0 (0.0)	1 (33.3)	0 (0.0)	1 (50.0)	0 (0.0)	1 (50.0)†	2 (100.0)	3 (3–6)
Restaurant	1 (0.6)	0 (0.0)	1 (100.0)	0 (0.0)	0 (0.0)	0 (0.0)	0 (0.0)	0 (0.0)	0 (0.0)	0 (100.0)	2
Total	176 (100.0)	84 (47.7)	42 (23.9)	10 (5.7)	40 (22.7)	83 (69.7)	33 (27.7)	1 (0.8)	2 (1.7)	119 (100.0)	3 (2–6)

Note: *M* (Q_1–Q_3)=Median.
* *S. sonnei* and *S. flexneri*.
† *S. flexneri* and *S. boydii*.

survival and proliferation. Regional variations in BD reporting requirements may also contribute to observed geographic patterns (*9*).

Schools emerged as the predominant setting for BD outbreaks. While previous studies have shown that peak BD case reporting typically occurs from June to September (*10*), this study's analysis revealed that outbreak reporting peaked in September and October, coinciding with school reopening after summer vacation. The return of students to campus environments increases outbreak risk by elevating bacterial exposure potential through shared facilities and close contact. Therefore, enhanced preventive management measures should be implemented before the academic year begins to mitigate outbreak risk.

Based on epidemiological investigations, this study identified the primary factors associated with outbreak occurrence. The high proportion of waterborne outbreaks aligns with previous findings that link consumable water contamination to disease transmission (*9*,*11*). Several schools faced challenges with regular disinfection of self-supplied water sources, while contaminated canteen storage reserves served as pathogen reservoirs, and many students consumed unboiled water. Schools should implement comprehensive water supply system management and monitoring, ensure student access to boiled or appropriately treated water, and promote awareness of safe drinking water practices. In foodborne outbreaks, *Shigella* carriage among school canteen staff represented a major cause of institutional outbreaks, emphasizing the critical need for regular health examinations and mandatory valid health certificates for food service personnel. Essential prevention strategies for foodborne outbreaks include enhanced hygiene education in food processing, proper utensil disinfection, strict separation of raw and cooked foods, and thorough cooking procedures.

Laboratory testing revealed that *S. sonnei* and *S. flexneri* caused most BD outbreaks, with *S. sonnei* predominating. This pattern contrasts with results from China's sentinel surveillance system, where *S. flexneri* dominates (*9*,*11*–*12*). This study's findings align with previous reports from China and other economically transitional countries (*13*), possibly due to the Type VI Secretion System (T6SS) encoded by *S. sonnei*, which enhances bacterial propagation and survival compared to *S. flexneri*, thereby increasing the propensity for *S. sonnei* to cause outbreaks (*14*).

Pathogen identification rates were substantially lower in other settings (46.3%) compared to school outbreaks (74.1%). Predominant pathogens varied by setting, with *S. sonnei* more prevalent in schools and *S. flexneri* in villages. These differences likely reflect environmental factors such as sanitation conditions, population exposure risks, and the biological characteristics of bacterial strains. *S. flexneri*, characterized by strong virulence, demonstrates better adaptation to environments with poor sanitation typical of rural villages, while *S. sonnei*, with weaker pathogenicity and milder symptoms, spreads more readily among children and adolescents. Its transmission is further facilitated by the densely populated school environment (*15*).

Outbreak magnitude varied significantly based on pathogen type and transmission route. Infections caused by *S. sonnei*, waterborne transmission, and prolonged outbreak duration were more likely to result

TABLE 2. Influencing factors on the outbreak size of bacillary dysentery in China, 2008–2024.

Variable	Outbreaks, *n* (%)	Univariate		Mutivariate	
		OR (95% *CI*)	*P*	a*OR* (95% *CI*)	*P*
Year					
2008–2013	113 (64.2)	1		1	
2014–2019	56 (31.8)	0.2 (0.02, 1.8)	0.16	0.2 (0.01, 1.7)	0.12
2020–2024	7 (4.0)	0.2 (0.02, 1.2)	0.08	0.2 (0.01, 1.4)	0.10
Area					
Urban	43 (24.4)	1		–	–
Rural	133 (75.6)	1.4 (0.7, 2.8)	0.34	–	–
Setting					
Other	8 (4.5)	1		1	
Kindergarden	18 (10.2)	4.5 (0.5, 44.4)	0.20	2.1 (0.1, 37.1)	0.61
Primary school	63 (35.8)	14.0 (1.6, 121.4)	0.02	8.3 (0.6, 122.1)	0.13
Middle/High school	42 (23.9)	8.5 (1.0, 75.2)	0.06	4.9 (0.3, 71.0)	0.24
Technical school/College	12 (6.8)	7.0 (0.7, 75.7)	0.11	7.8 (0.4, 150.4)	0.18
Village	33 (18.8)	3.0 (0.3, 28.1)	0.33	2.9 (0.2, 45.4)	0.44
Route of transmission					
Unknown	40 (22.7)	1		1	
Water-borne	84 (47.7)	5.0 (2.2, 11.4)	<0.001	5.4 (1.9, 15.3)	0.001
Food-borne	42 (23.9)	2.4 (1.0, 6.0)	0.06	2.6 (0.9, 7.7)	0.09
Contact-borne	10 (5.7)	1.1 (0.3, 5.2)	0.88	1.8 (0.3, 11.4)	0.54
Response time, days					
≤3	78 (44.3)	1		1	
4–7	56 (31.8)	0.6 (0.3, 1.2)	0.14	0.3 (0.1, 0.8)	0.01
≤8	42 (23.9)	0.4 (0.2, 0.9)	0.02	0.3 (0.1, 1.1)	0.07
Duration, days					
≤3	33 (18.8)	1		1	
4–7	62 (35.2)	2.1 (0.9, 5.0)	0.09	2.9 (1.0, 8.5)	0.05
≤8	81 (46.0)	1.5 (0.7, 3.4)	0.33	3.8 (1.0, 13.8)	0.04
Pathogen					
Unclassified	57 (32.4)	1		1	
Shigella sonnei	83 (47.2)	4.2 (2.0, 8.5)	<0.001	4.3 (1.7, 10.9)	0.002
Shigella flexneri	33 (18.8)	1.1 (0.5, 2.8)	0.77	1.5 (0.5, 4.5)	0.44
Shigella boydii/Mixed infection	3 (1.7)	4.0 (0.3, 47.0)	0.27	6.8 (0.3, 138.4)	0.21

Note: - indicates that the variable was not included in the multivariable model.
Abbreviation: a*OR*=adjusted odds ratios; *CI*=confidence interval.

in large-scale outbreaks. These findings emphasize the critical importance of enhanced drinking water management and the development of healthy consumption habits, particularly avoiding raw water consumption. Furthermore, strengthening surveillance systems and ensuring prompt reporting help reduce epidemic scale, while enhancing laboratory testing capabilities deepens the understanding of epidemiological patterns and antimicrobial resistance profiles, thereby guiding appropriate treatment strategies and reducing BD burden.

This study has several limitations. The data originated from a passive surveillance system, which may have underestimated outbreak frequency due to unreported, undiagnosed, or misdiagnosed cases. Delayed detection can cause reporting delays, while limitations in surveillance sensitivity and geographical coverage may further contribute to missed outbreaks.

In conclusion, this study conducted a comprehensive analysis of BD outbreak characteristics and response measures in China from 2008 to 2024. China has achieved considerable success in controlling bacillary dysentery through effective prevention strategies, with a significant decline in outbreak frequency. China's experience in bacillary dysentery control can provide valuable insights for other developing countries facing similar public health challenges.

Conflicts of interest: No conflicts of interest.

Acknowledgements: Sincere gratitude to Lance Rodewald, Senior Advisor at the Chinese Center for Disease Control and Prevention, for his meticulous proofreading and expert language refinement that significantly enhanced the readability and clarity of our manuscript.

doi: 10.46234/ccdcw2025.177

Corresponding author: Zhaorui Chang, changzr@chinacdc.cn.

[1] Chinese Field Epidemiology Training Program, Chinese Center for Disease Control and Prevention, Beijing, China; [2] Guangdong Center for Disease Control and Prevention, Guangzhou City, Guangdong Province, China; [3] National Key Laboratory of Intelligent Tracking and Forecasting for Infectious Diseases, Division of Infectious Disease, Chinese Center for Disease Control and Prevention, Beijing, China.

Submitted: June 16, 2025
Accepted: August 01, 2025
Issued: August 08, 2025

REFERENCES

1. Kotloff KL, Riddle MS, Platts-Mills JA, Pavlinac P, Zaidi AKM. Shigellosis. Lancet 2018;391(10122):801 – 12. https://doi.org/10.1016/S0140-6736(17)33296-8.
2. GBD Diarrhoeal Diseases Collaborators. Estimates of global, regional, and national morbidity, mortality, and aetiologies of diarrhoeal diseases: a systematic analysis for the global burden of disease study 2015. Lancet Infect Dis 2017;17(9):909 – 48. https://doi.org/10.1016/S1473-3099(17)30276-1.
3. Zhang YF, Liu FF, Song Y, Qin T, Jin Dong, Chang ZR, et al. Epidemiological characteristics of bacillary dysentery in China, 2005-2024[J]. Chin J Epidemiol, 2025, 46(6):942-50. http://doi.org/10.3760/cma.j.cn112338-20250311-00153.
4. Jing ZM, Ma T, Feng Z, Hong L, Zhou L, Ma HL, et al. Outbreak investigation of bacterial dysentery in two colleges in Nanjing. Chin J Hyg Rescue (Electron Ed) 2016;2(6):358 – 64. https://doi.org/10.3877/cma.j.issn.2095-9133.2016.06.005.
5. Lyu B, Tian Y, Yang YN, Zhen BJ, Jia L, Lin CY, et al. Etiological analysis on a bacillary dysentery outbreak caused by *Shigella sonnei* in Beijing. Dis Surveill 2022;37(1):139 – 43. (In Chinese). https://doi.org/10.3784/jbjc.202103020099.
6. Pan JJ, Liu XW. Analysis of the epidemiological characteristics of bacillary dysentery in China from 2005 to 2017. Chin Health Ind 2021;18(19):166 – 72. https://doi.org/10.16659/j.cnki.1672-5654.2021.19.166.
7. Geng MJ, Zhang HY, Yu LJ, Lv CL, Wang T, Che TL, et al. Changes in notifiable infectious disease incidence in China during the COVID-19 pandemic. Nat Commun 2021;12(1):6923. https://doi.org/10.1038/s41467-021-27292-7.
8. Wang XF, Zhang YW, Shi QN. Spatial distribution of hot spots of bacterial dysentery and related environmental factors in Southwestern China. Dis Surveill 2018;33(7):573 – 9. https://doi.org/10.3784/j.issn.1003-9961.2018.07.010.
9. Chang ZR, Zhang J, Zhang WD, Sun JL. Analysis on bacillary dysentery outbreaks in China, 2008-2011. Chin J Food Hyg 2012;24(6):554 – 8. https://doi.org/10.13590/j.cjfh.2012.06.018.
10. Chang ZR, Zhang J, Ran L, Sun JL, Liu FF, Luo L, et al. The changing epidemiology of bacillary dysentery and characteristics of antimicrobial resistance of *Shigella* isolated in China from 2004–2014. BMC Infect Dis 2016;16(1):685. https://doi.org/10.1186/s12879-016-1977-1.
11. Chang ZR, Sun QZ, Pei YX, Zhang J, Sun JL. Surveillance for bacillary dysentery in China, 2012. Dis Surveill 2014;29(7):528 – 32. https://doi.org/10.3784/j.issn.1003-9961.2014.07.006.
12. Ohlsen EC, Angel K, Maroufi A, Kao AN, Victorio MJ, Cua LS, et al. Shigellosis outbreak among persons experiencing homelessness-San Diego County, California, October-December 2021. Epidemiol Infect 2023;152:e61. https://doi.org/10.1017/S0950268823001681.
13. Baker S, The HC. Recent insights into *Shigella*: a major contributor to the global diarrhoeal disease burden. Curr Opin Infect Dis 2018;31(5):449 – 54. https://doi.org/10.1097/QCO.0000000000000475.
14. Anderson MC, Vonaesch P, Saffarian A, Marteyn BS, Sansonetti PJ. *Shigella sonnei* encodes a functional T6SS used for interbacterial competition and niche occupancy. Cell Host Microbe 2017;21(6):769 – 76.e3. https://doi.org/10.1016/j.chom.2017.05.004.
15. Shad AA, Shad WA. *Shigella sonnei*: virulence and antibiotic resistance. Arch Microbiol 2021;203(1):45 – 58. https://doi.org/10.1007/s00203-020-02034-3.

Preplanned Studies

Co-harboring *bla*$_{KPC-2}$ and *bla*$_{IMP-4}$ on an IncP Plasmid in A Clinical Isolate of *Klebsiella pneumoniae* — Shanghai Municipality, China, 2023

Meng Wang[1,&]; Jumao Huang[2,&]; Dai Kuang[3,&]; Jieming Qu[2]; Cui Tai[1,#]

Summary

What is already known about this topic?

Carbapenem-resistant *Klebsiella pneumoniae* (CRKP) poses a major threat to global health. The co-production of multiple carbapenemases has emerged as a critical concern, further limiting the effectiveness of last-resort antibiotics such as ceftazidime-avibactam.

What is added by this report?

This study identifies an IncP6 plasmid co-harboring both *bla*$_{KPC-2}$ and *bla*$_{IMP-4}$ in a clinical isolate of *K. pneumoniae*. Comprehensive genomic analysis reveals a complex plasmid structure shaped by recombination events and highlights its potential for mobilization, underscoring the heightened risk of carbapenem resistance.

What are the implications for public health practice?

The emergence and diversification of plasmids co-harboring distinct carbapenemase genes highlight the urgent need for comprehensive genomic surveillance, stringent infection control protocols, and judicious antimicrobial management. These measures are essential to curtail the spread and evolution of multidrug-resistant organisms, which pose a substantial threat to public health globally.

ABSTRACT

Introduction: Carbapenem-resistant *Klebsiella pneumoniae* (CRKP) poses a significant global public health threat. The dissemination of resistance is accelerated by plasmids harboring multiple carbapenemase genes, posing a particular challenge to the limited treatment options, including ceftazidime-avibactam.

Methods: In this study, a CRKP strain, KpBSI024, was isolated from a patient with bloodstream infection in the intensive care unit of a tertiary hospital in China. The whole-genome sequencing combined with bioinformatic analysis was used to investigate the structural features of plasmids and associated resistance genes. In addition, conjugation experiments were conducted to assess the transferability of the resistance plasmid.

Results: KpBSI024 exhibited resistance to carbapenems and ceftazidime-avibactam and was identified as sequence type ST1514. Whole-genome sequencing revealed that two carbapenemase genes, *bla*$_{KPC-2}$ and *bla*$_{IMP-4}$, coexisted on a 53 kb IncP6-type plasmid. This plasmid exhibited a complex structure, likely formed through multiple recombination events mediated by IS*26* between plasmids of different Inc types. Although the resistance plasmid encodes a type IV secretion system, it lacks a relaxase gene and is therefore non-self-transmissible; however, it could be transferred at low frequency to *Escherichia coli* with the assistance of a conjugative plasmid. The growth of the transconjugants was not affected by the acquisition of the resistance plasmid, and they displayed resistance profiles to carbapenems and ceftazidime-avibactam similar to the donor strain.

Conclusions: The coexistence of *bla*$_{KPC-2}$ and *bla*$_{IMP-4}$ on an IncP-type plasmid in a clinical *K. pneumoniae* isolate highlights the critical role of recombination events in the dissemination of resistance genes. The emergence of such multidrug-resistant plasmids underscores the urgent need for genomic surveillance and the development of innovative antimicrobial strategies to control the spread of high-risk resistance plasmids.

The worldwide prevalence of carbapenem-resistant *Klebsiella pneumoniae* (CRKP) presents a significant public health challenge. The major carbapenemases include KPC (class A), IMP, VIM, and NDM (class B), and OXA-48 (class D), all of which contribute to nosocomial outbreaks. Recent findings have

highlighted the emergence of clinical isolates co-producing multiple carbapenemases, further complicating the already limited therapeutic options (*1*). This phenomenon is associated with various plasmid-borne carbapenemase genes. Among them, IncP plasmids are notable for their broad host range, high conjugation efficiency, and frequent carriage of resistance genes, facilitating widespread dissemination and microbial adaptation through mobile genetic elements and recombination hotspots (*2*). In this study, a novel IncP6 plasmid that concurrently harbors the $bla_{\text{KPC-2}}$ and $bla_{\text{IMP-4}}$ genes in a *K. pneumoniae* clinical isolate was identified and designated as KpBSI024.

The strain KpBSI024 was isolated in 2023 from a patient with a bloodstream infection admitted to an intensive care unit (ICU) at a tertiary hospital in Shanghai, China, as part of a surveillance study. Antimicrobial susceptibility testing revealed resistance to β-lactam/β-lactam inhibitors and carbapenems, with MICs of 16 μg/mL for both meropenem and imipenem, and reduced susceptibility to ceftazidime-avibactam (Table 1). Whole-genome sequencing using Illumina and Nanopore platforms (Supplementary Methods) revealed that KpBSI024 belongs to ST1514 and KL109, a rare lineage previously associated only with carbapenem-susceptible *K. pneumoniae* (*3*). The genome comprised a chromosome and five plasmids (IncFIB, IncFII, IncQ1, IncP6, and Col440I), with $bla_{\text{KPC-2}}$ and $bla_{\text{IMP-4}}$ co-located on the IncP6 plasmid pKpBSI024-3 (Figure 1A). In addition, KpBSI024 harbors the aminoglycoside resistance genes *aac(3)-IId, aac(6')-Ib-cr*, *aadA16, aph(3')-Ia*, *aph(3'')-Ib*, and *aph(6)-Id*; β-lactam resistance genes $bla_{\text{CTX-M-3}}$, $bla_{\text{SHV-61}}$, $bla_{\text{TEM-1A}}$, and $bla_{\text{TEM-1B}}$; rifamycin resistance gene *ARR-3*; amphenicol resistance gene

TABLE 1. Antimicrobial susceptibility profiles of CRKP KpBSI024 and other strains used in the transfer assay of the resistant plasmid pKpBSI024-3 (p3)*.

Antimicrobial agent†	Antimicrobial susceptibility results (MIC, μg/mL)§				
	***K. pneumoniae* KpBSI024**	***K. pneumoniae* KpBSI024-p0**	***E. coli* C600-pA**	***E. coli* C600-pA-p0-p3**	***E. coli* ATCC 25922¶**
Aztreonam	≥64 (R)	32 (R)	≤1 (S)	≥64 (R)	≤1 (S)
Imipenem	≥16 (R)	≥16 (R)	≤0.25 (S)	≥16 (R)	≤0.25 (S)
Meropenem	≥16 (R)	8 (R)	≤0.25 (S)	≥16 (R)	≤0.25 (S)
Cefepime	≥32 (R)	≥32 (R)	≤0.12 (S)	≥32 (R)	≤0.12 (S)
Ceftazidime	≥64 (R)	≥64 (R)	0.5 (S)	≥64 (R)	≤0.12 (S)
Ceftazidime-avibactam	64/4 (R)	32/4 (R)	0.25/4 (S)	128/4 (R)	≤0.12 (S)
Cefoperazone-sulbactam	≥64 (R)	≥64 (R)	≤8 (S)	≥64 (R)	≤8 (S)
Ticarcillin-clavulanate	≥128 (R)	≥128 (R)	≤8 (S)	≥128 (R)	≤8 (S)
Piperacillin-tazobactam	≥128 (R)	≥128 (R)	8 (S)	≥128 (R)	≤4 (S)
Trimethoprim-sulfamethoxazole	≥320 (R)	≥320 (R)	≤20 (S)	≤20 (S)	≤20 (S)
Amikacin	≤2 (S)	≤2 (S)	≤2 (S)	≤2 (S)	4 (S)
Tobramycin	8 (I)	8 (I)	≥16 (R)	≥16 (R)	≤1 (S)
Ciprofloxacin	≥4 (R)	≥4 (R)	≤0.25 (S)	≥4 (R)	≤0.25 (S)
Levofloxacin	≥8 (R)	≥8 (R)	0.5 (S)	4 (R)	≤0.12 (S)
Doxycycline	≥16 (R)	≥16 (R)	≥16 (R)	≥16 (R)	≤0.5 (S)
Minocycline	4 (S)	8 (I)	8 (I)	4 (S)	≤1 (S)
Tigecycline	≤0.5 (S)	1 (S)	1 (S)	≤0.5 (S)	≤0.5 (S)
Polymyxin	1 (S)	≤0.5 (S)	2 (S)	≤0.5 (S)	≤0.5 (S)

Abbreviation: MIC=minimum inhibitory concentration; R=resistant; S=susceptible; I=intermediate; CRKP=carbapenem-resistant *Klebsiella pneumoniae*; *E. coli=Escherichia coli*; CLSI=Clinical and Laboratory Standards Institute.

* The clinical isolate of CRKP KpBSI024 contains the mobilizable plasmid pKpBSI024-3 (p3) co-harboring $bla_{\text{KPC-2}}$ and $bla_{\text{IMP-4}}$. The strain information is provided in Supplementary Figure S1 and Supplementary Table S1 (available at https://weekly.chinacdc.cn/).

† The MIC was determined by the VITEK2 Compact system except for ceftazidime-avibactam. The MIC of ceftazidime-avibactam was determined using the microbroth dilution method.

§ Bacterial antimicrobial susceptibility was interpreted based on the CLSI guidelines 2025 (M100).

¶ *E. coli* ATCC 25922 was used as the quality control strain.

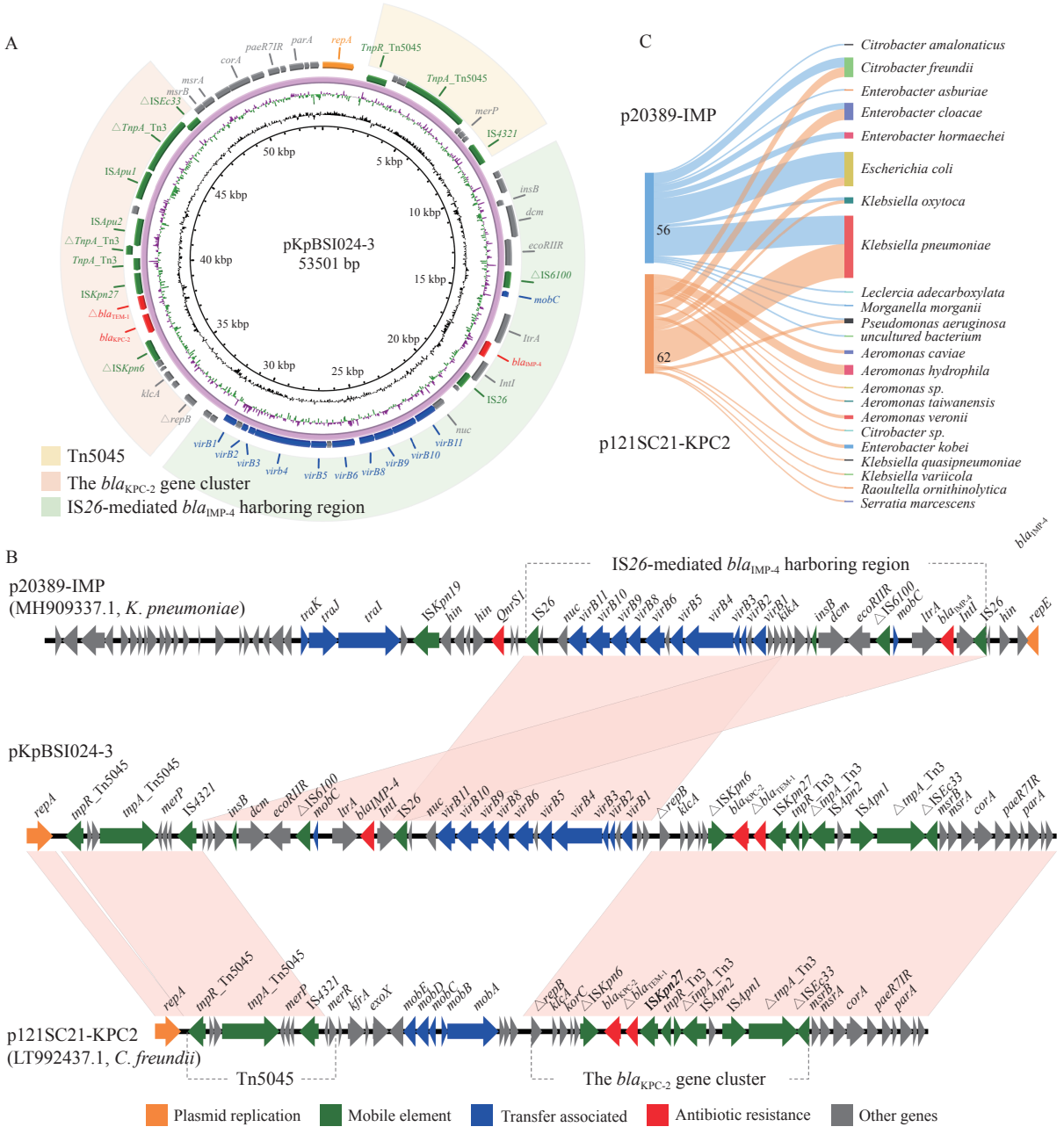

FIGURE 1. Organizational schematic of the bla_{KPC-2} and bla_{IMP-4}-carrying plasmid pKpBSI024-3 from the *K. pneumoniae* clinical isolate KpBSI024. (A) Plasmid map annotated by gene function; (B) Linear comparison of pKpBSI024-3 with reference plasmids p121SC21-KPC2 and p20389-IMP; (C) Bacterial hosts carrying similar plasmids with >90% coverage and >99% identity.
Note: For (A), orange: replication; green: mobile elements; blue: transfer; red: resistance; For (C), based on NCBI *nr* database analysis.

floR; quinolone resistance genes *qnrS1, qnrB91, OqxA, OqxB*, and *mdf(A)*; folate pathway antagonist resistance genes *sul1, sul2*, and *dfrA27*; tetracycline resistance gene *tet(A)*; macrolide resistance gene *mph(A)*; and fosfomycin resistance gene *fosA*.

VRprofile2 analysis indicated that pKpBSI024-3 encodes a type IV secretion system but lacks the relaxase gene and chaperone protein, which are essential for conjugation (Figure 1B). Attempts to transfer pKpBSI024-3 from *K. pneumoniae* KpBSI024 into *E. coli* (C600-pA) via conjugation were unsuccessful. However, the mobilization of pKpBSI024-3 was achieved at a frequency of $(2.51\pm2.00)\times10^{-7}$ using the helper conjugative plasmid

pKP2648-34 (Supplementary Material, Supplementary Tables S1–S2, and Supplementary Figure S1, available at https://weekly.chinacdc.cn/). The self-transmissible pKP2648-34, which is 34 kb in size and lacks any antibiotic resistance genes (*4*), was first introduced into KpBSI024. Following acquisition of the pKpBSI024-3 plasmid, *E. coli* (C600-pA) exhibited resistance to carbapenems and ceftazidime-avibactam similar to the donor strain KpBSI024 (Table 1). Growth curve analysis demonstrated that transfer of the 53-kb plasmid pKpBSI024-3 did not impose a substantial metabolic burden on the recipient strain (Supplementary Figure S2, available at https://weekly.chinacdc.cn/).

Comparative genomic analysis revealed that pKpBSI024-3 originated through recombination between two plasmids: IncP6 plasmid p121SC21-KPC2 (55% coverage, 100% identity) (*5*) and IncN plasmid p20389-IMP (43% coverage, 99.99% identity) (*6*) (Figure 1B). Sequence analysis indicated a complex mosaic arrangement, wherein the $bla_{\text{KPC-2}}$ gene resides within a Tn3-based transposon exhibiting a disrupted structure (ΔIS*Ec33*-Tn*3*-IS*Apu1*-orf-IS*Apu2*-IS*Kpn27*-Δ$bla_{\text{TEM-1}}$-$bla_{\text{KPC-2}}$-ΔIS*Kpn6*-*korC*-*klcA*-Δ*repB*). This structure resembles the Tn*1722* transposon unit, a major vehicle for $bla_{\text{KPC-2}}$ dissemination frequently identified in China, characterized by the conserved *ISKpn27*-$bla_{\text{KPC-2}}$-Δ*ISKpn6* core. However, unlike typical Tn*1722*, this variant lacks the *tnpR* and *tnpA* transposition genes, and includes multiple additional insertion sequences (e.g., IS*Apu1*, IS*Apu2*, and IS*Ec33*). These findings suggest that sequential insertion events and extensive structural rearrangements contributed to the current mosaic architecture of pKpBSI024-3. Meanwhile, the $bla_{\text{IMP-4}}$ gene is embedded within a class 1 integron associated with IS*26*. Additional mobile genetic elements, including Tn*5045* and IS*4321*, further emphasize the complexity of the plasmid's recombination processes. Based on these findings, it was hypothesized that pKpBSI024-3 was formed through a multi-step recombination process. Initially, the IS*26*-flanked region containing $bla_{\text{IMP-4}}$ was excised from p20389-IMP via IS*26*-mediated homologous recombination, forming a circular intermediate. This structure subsequently integrated into the backbone of p121SC21-KPC2. Notably, this insertion event appeared to be accompanied by deletion of a contiguous region associated with conjugative transfer, resulting in a rearranged backbone.

Furthermore, it is notable that the two plasmids involved in the recombination event leading to pKpBSI024-3 exhibit differing transfer capabilities. The plasmid p20389-IMP is self-transmissible, whereas p121SC21-KPC2 contains a mobilization module (*mobA-mobE*) and may transfer with the assistance of a conjugative plasmid (Figure 1B). Additionally, genomic comparisons with p121SC21-KPC2 and p20389-IMP from the NCBI *nr* database revealed highly similar plasmids across multiple bacterial hosts and datasets. p20389-IMP has 56 similar plasmids, while p121SC21-KPC2 has 62. These exhibited >90% query coverage and >99% nucleotide identity (Figure 1C). The bacterial hosts involved primarily include *K. pneumoniae*, *E. coli*, and *C. freundii*, spanning more than 20 species. Their distribution is geographically diverse, encompassing more than nine countries, with a significant prevalence in China and Spain (Supplementary Table S3, available at https://weekly.chinacdc.cn/). The widespread presence of these highly similar plasmids highlights the potential for recombination and the associated risk of broad dissemination.

DISCUSSION

The identification of *K. pneumoniae* KpBSI024 harboring an IncP6 plasmid containing both $bla_{\text{KPC-2}}$ and $bla_{\text{IMP-4}}$ represents a notable advancement in our understanding of multidrug resistance evolution. Although KPC and IMP carbapenemase genes have been individually associated with various plasmid replicon types, including IncP-type plasmids, this is the first report of their co-localization within a single IncP plasmid. In contrast to prior studies documenting IncP plasmids carrying bla_{IMP} in *Pseudomonas* or bla_{KPC} variants in *Klebsiella* (*7*–*8*), this study highlights a novel evolutionary convergence, underscoring the increased recombination capacity and heightened risk of multidrug resistance. Furthermore, this finding differs from the recently characterized IncN-IncR plasmid co-harboring bla_{KPC} and bla_{IMP} in *K. pneumoniae* ST1393, where recombination was facilitated by IS*Kpn19* and IS*Kpn27* (*9*). These observations emphasize the evolutionary pressures driving plasmid recombination and the emergence of complex resistance mechanisms. Despite the requirement for a helper conjugative plasmid to facilitate mobilization of pKpBSI024-3, its genomic resemblance to plasmids identified across diverse bacterial hosts suggests the potential for widespread

dissemination.

Plasmid pKpBSI024-3 exemplifies the importance of recombination in promoting genetic diversity among resistance determinants. The interplay of Tn*3*-based transposons, IS*26*-associated integrons, and multiple IS elements likely contributed to the integration of resistance genes from various plasmid sources. Such mosaic plasmids pose a considerable threat to antimicrobial treatment, as the co-expression of serine- and metallo-carbapenemases can synergistically compromise the efficacy of available therapies, including next-generation inhibitors such as ceftazidime-avibactam.

From an epidemiological standpoint, the ST1514 lineage remains relatively rare, with prior reports predominantly involving carbapenem-susceptible isolates. The acquisition of a high-risk plasmid such as pKpBSI024-3 may signify a potential shift toward multidrug resistance within this lineage. The limited conjugation observed under laboratory conditions contrasts with the widespread detection of similar plasmids in diverse bacterial hosts, implying possible alternative mechanisms of horizontal gene transfer or environmental adaptation.

The extensive repertoire of resistance genes present on pKpBSI024-3, including those mediating resistance to β-lactams, aminoglycosides, quinolones, and fosfomycin, illustrates the therapeutic difficulties associated with such plasmids. The observed resistance to ceftazidime-avibactam is particularly concerning, as this agent constitutes one of the few remaining treatment options for CRKP infections. The potential for interspecies plasmid transfer further exacerbates these concerns.

The public health implications of such plasmids are profound, as they undermine the efficacy of critical antimicrobial agents and complicate infection control strategies. Continuous surveillance of high-risk plasmids and their derivatives should be prioritized. Moreover, there is an urgent need for novel therapeutic strategies to combat plasmid-mediated multidrug resistance. One promising approach involves the development of CRISPR-Cas-based systems engineered to selectively eliminate resistant plasmids (*10*).

In conclusion, the identification of the IncP6 plasmid co-harboring $bla_{\text{KPC-2}}$ and $bla_{\text{IMP-4}}$ exemplifies the dynamic nature of resistance gene dissemination in *K. pneumoniae*. The public health implications of such plasmids are substantial. Genomic surveillance efforts should prioritize the detection of plasmid-mediated resistance genes, particularly those capable of co-harboring multiple carbapenemases. Rigorous monitoring of plasmid dynamics and resistance gene transmission is essential to prevent the emergence of untreatable infections. Additionally, the development of novel therapeutic strategies targeting plasmid stability and mobility may offer promising approaches to mitigate the spread of multidrug resistance.

Conflicts of interest: No conflicts of interest.

Ethical statement: Approved by the Ethics Committee of Ruijin Hospital, School of Medicine, Shanghai Jiao Tong University (No. RJ2019NO1-3).

Funding: Supported by the National Key Research and Development Program of China (2024YFE0199000) , the National Natural Science Foundation of China (82000011), Hainan Provincial Natural Science Foundation of China (825RC764) and the Decision-Making Consultation Project of Shanghai Jiao Tong University (JCZXSJB2023-13).

doi: 10.46234/ccdcw2025.178

[#] Corresponding author: Cui Tai, ctai@sjtu.edu.cn.

[1] State Key Laboratory of Microbial Metabolism, School of Life Sciences & Biotechnology, Shanghai Jiao Tong University, Shanghai, China; [2] Department of Pulmonary and Critical Care Medicine, Ruijin Hospital, Shanghai Jiao Tong University School of Medicine, Shanghai, China; [3] School of Tropical Medicine, Hainan Medical University, Haikou City, Hainan Province, China.
[&] Joint first authors.

Submitted: May 14, 2025
Accepted: August 01, 2025
Issued: August 08, 2025

REFERENCES

1. Gao H, Liu YD, Wang RB, Wang Q, Jin LY, Wang H. The transferability and evolution of NDM-1 and KPC-2 co-producing *Klebsiella pneumoniae* from clinical settings. EBioMedicine 2020;51: 102599. https://doi.org/10.1016/j.ebiom.2019.102599.
2. Popowska M, Krawczyk-Balska A. Broad-host-range IncP-1 plasmids and their resistance potential. Front Microbiol 2013;4:44. https://doi.org/10.3389/fmicb.2013.00044.
3. Gomez-Simmonds A, Greenman M, Sullivan SB, Tanner JP, Sowash MG, Whittier S, et al. Population structure of *Klebsiella pneumoniae* causing bloodstream infections at a New York City tertiary care hospital: diversification of multidrug-resistant isolates. J Clin Microbiol 2015;53(7):2060 – 7. https://doi.org/10.1128/jcm.03455-14.
4. Wang XL, Tang B, Liu GT, Wang M, Sun JY, Tan RM, et al. Transmission of nonconjugative virulence or resistance plasmids mediated by a self-transferable IncN3 plasmid from carbapenem-resistant *Klebsiella pneumoniae*. Microbiol Spectr 2022;10(4):e0136422. https://doi.org/10.1128/spectrum.01364-22.
5. Ghiglione B, Haim MS, Penzotti P, Brunetti F, D´Amico González G,

Di Conza J, et al. Characterization of emerging pathogens carrying *bla*$_{KPC}$-2 gene in IncP-6 plasmids isolated from urban sewage in Argentina. Front Cell Infect Microbiol 2021;11:722536. https://doi.org/10.3389/fcimb.2021.722536.

6. Lo WU, Cheung YY, Lai E, Lung D, Que TL, Ho PL. Complete sequence of an IncN plasmid, pIMP-HZ1, carrying *bla*$_{IMP}$-4 in a *Klebsiella pneumoniae* strain associated with medical travel to China. Antimicrob Agents Chemother 2013;57(3):1561 – 2. https://doi.org/10.1128/AAC.02298-12.
7. Zhang XF, Wang LL, Li D, Li P, Yuan LL, Yang F, et al. An IncP-2 plasmid sublineage associated with dissemination of *bla*$_{IMP}$-45 among carbapenem-resistant *Pseudomonas aeruginosa*. Emerg Microbes Infect 2021;10(1):442 – 9. https://doi.org/10.1080/22221751.2021.1894903.
8. Ota Y, Prah I, Nukui Y, Koike R, Saito R. *bla*$_{KPC}$-2-encoding IncP-6 plasmids in *Citrobacter freundii* and *Klebsiella variicola* strains from hospital sewage in Japan. Appl Environ Microbiol 2022;88(8):e0001922. https://doi.org/10.1128/aem.00019-22.
9. Fang L, Shen YH, Chen RY, Li CY, Liu RS, Jia YY, et al. The characterization of an IncN-IncR fusion plasmid co-harboring *bla*$_{TEM-40}$, *bla*$_{KPC-2}$, and *bla*$_{IMP-4}$ derived from ST1393 *Klebsiella pneumoniae*. Sci Rep 2024;14(1):26723. https://doi.org/10.1038/s41598-024-78205-9.
10. Mayorga-Ramos A, Zúñiga-Miranda J, Carrera-Pacheco SE, Barba-Ostria C, Guamán LP. CRISPR-Cas-based antimicrobials: design, challenges, and bacterial mechanisms of resistance. ACS Infect Dis 2023;9(7):1283 – 302. https://doi.org/10.1021/acsinfecdis.2c00649.

SUPPLEMENTARY MATERIAL

Whole-genome Sequencing, Assembly, and Annotation

Genomic DNA from the carbapenem-resistant *Klebsiella pneumoniae* (CRKP) isolate KpBSI024 was extracted and subjected to both short-read and long-read sequencing using the Illumina HiSeq and Oxford Nanopore MinION platforms, respectively. For Illumina data, read quality was assessed using FastQC, and low-quality bases and adapter sequences were trimmed with fastp (v0.24.0) (*1*), achieving a Q30 > 99%. For Nanopore data, reads shorter than 1 kb were excluded. Hybrid genome assembly was conducted with Unicycler (v0.5.0) (*2*) using default parameters, in which high-quality Illumina reads were used to polish Nanopore reads to enhance assembly accuracy. All chromosomes and plasmids were circularized, confirming complete assembly. Genome annotation was performed using Prokka (v1.12) (*3*), while functional profiling, including antimicrobial resistance gene (ARG) identification, plasmid replicon typing, and detection of mobile genetic elements, was carried out using VRprofile2 (*4*). This tool internally runs Abricate (https://github.com/tseemann/abricate) with the ResFinder (v4.6.0) (*5*) and PlasmidFinder (v2.0.1) (*6*) databases, applying ≥80% coverage and ≥80% identity thresholds. All identified ARGs exhibited >90% coverage and identity. Sequence typing was performed using MLST (v2.0.9) (*7*). Additional analyses utilized BRIG (v0.95) (*8*) and EasyFig (v3.0.0) (*9*).

Bacterial Strains and Conjugation Assays

Antimicrobial susceptibility testing was performed in accordance with Clinical and Laboratory Standards Institute (CLSI) guidelines (*10*). *K. pneumoniae* KpBSI024 and *E. coli* C600 were used for conjugation assays (Supplementary Figure S1). The *E. coli* C600-p0 and C600-pA strains were obtained from previous studies (*11–12*). Detailed information on bacterial strains and plasmids is provided in Supplementary Table S1; primer sequences are listed in Table S2. All strains were cultured in lysogeny broth (LB) at 37 °C with appropriate antibiotics. Conjugation assays were conducted as previously described (*11*). Briefly, overnight cultures of donor and recipient strains were diluted 1:100 in fresh LB medium and incubated at 220 rpm and 37 °C. When cultures reached an OD_{600} of 0.6, 1 mL of each donor and recipient culture was harvested, washed with PBS, resuspended in 100 μL of 10 mmol/L $MgSO_4$ mixed at a 1:1 ratio, and spotted 20 μL mixed cells onto pre-warmed LB agar plates. After overnight incubation at 37 °C, cells were recovered, resuspended in LB medium, serially diluted, and plated on LB agar containing selective antibiotics. When KpBSI024 was the recipient for selection, plates contained 50 μg/mL ceftazidime-avibactam. To select for transconjugants acquiring pKpBSI024-3 in *E. coli* C600-pA, plates contained 50 μg/mL ceftazidime-avibactam, 50 μg/mL apramycin, and 100 μg/mL rifamycin. For transconjugants carrying pKP2648-34, plates contained 200 μg/mL hygromycin, 50 μg/mL apramycin, and 100 μg/mL rifamycin. Following overnight incubation, colony-forming units (CFUs) were enumerated. Transconjugants were confirmed by PCR, and conjugation frequency was calculated as the number of confirmed transconjugants divided by the total

SUPPLEMENTARY TABLE S1. Bacterial strains and plasmids used in this study.

Strain/Plasmid	Note	Source
Strain		
KpBSI024	*K. pneumoniae*, ST1514, bla_{KPC-2}+, bla_{IMP-4}+, Mem^R, CAZ^R	This study
KpBSI024-p0	*K. pneumoniae*, Transconjugant carrying p0 from C600-p0, Mem^R, CAZ^R	This study
C600-p0	*E. coli*, Transconjugant carrying p0 from KP2648, Rif^R	Wang, et al. (*12*)
C600-pA	*E. coli*, Recipient in the conjugation assay, Apr^R, Rif^R	Zhang, et al. (*11*)
C600-pA-p0-p3	*E. coli*, Transconjugant carrying p0, p3 and pACYC184-Apr; Mem^R, CAZ^R, Apr^R, Rif^R	This study
Plasmid		
p3 (pKpBSI024-3)	Mobilizable, natural plasmid in CRKP KpBSI024, bla_{KPC-2}+, bla_{IMP-4}+	This study
p0 (pKP2648-34)	Conjugative, helper plasmid in KP2648 with *hph* insertion, Hm^R	Wang, et al. (*12*)
pA (pACYC184-Apr)	Non-mobilizable, p15A origin of replication, Apr^R	Bartolomé, et al. (*13*)

Abbreviation: CRKP=carbapenem-resistant *Klebsiella pneumoniae*; Apr^R=apramycin resistance; Hm^R=hygromycin resistance; CAZ^R=ceftazidime-avibactam resistance; Rif^R=rifampicin resistance; Mem^R=meropenem resistance.

SUPPLEMENTARY TABLE S2. Oligonucleotide primers used in this study.

Name	Sequence (5'–3')	Description
C600-F	GGGCAAACTCACTCAATTTCTGG	Validation *E. coli* C600
C600-R	CATATCCATCGCCCGGAATATGAAT	
KpBSI024-F	ATGGCTGGTGGTACAGGTAG	Validation *K. pneumoniae* KpBSI024
KpBSI024-R	CGCGTTGGATATAACCATAGCC	
pKpBSI024-3-F	CGTCTAGTTCTGCTGTCTTG	Validation plasmid pKpBSI024_3
pKpBSI024-3-R	CTTGTCATCCTTGTTAGGCG	
pKP2648-34-F	GATACCCTGGCCTTTTAGCC	Validation plasmid pKP2648_34
pKP2648-34-R	TTGACGAAGCAGGGGTAATC	

SUPPLEMENTARY TABLE S3. Distribution of plasmids similar to p20389-IMP and p121SC21-KPC2 identified in the NCBI *nr* database.

Query	Target	Target species	Target length	Query cover (%)	Identities (%)	E value	Collection date	Geographic location
LT992437.1	OW849094.1	*Enterobacter cloacae*	40,714	100	100.00	0	2016	Spain
LT992437.1	CP110880.1	*Enterobacter kobei*	42,506	100	100.00	0	2019/08	China
LT992437.1	OW969881.1	*Citrobacter freundii*	41,032	100	99.99	0	2016	Spain
LT992437.1	OW849032.1	*Raoultella ornithinolytica*	40,356	100	99.99	0	2016	Spain
LT992437.1	OW970224.1	*Klebsiella pneumoniae*	40,441	100	99.98	0	2016	Spain
LT992437.1	OW969860.1	*Klebsiella pneumoniae*	40,441	100	99.98	0	2015	Spain
LT992437.1	OW968457.1	*Klebsiella pneumoniae*	40,730	100	99.98	0	2015	Spain
LT992437.1	OW968248.1	*Klebsiella pneumoniae*	40,424	100	99.98	0	2016	Spain
LT992437.1	OW968211.1	*Klebsiella pneumoniae*	40,509	100	99.98	0	2016	Spain
LT992437.1	OW968195.1	*Klebsiella pneumoniae*	40,815	100	99.98	0	2015	Spain
LT992437.1	OW849136.1	*Klebsiella oxytoca*	40,441	100	99.98	0	2018	Spain
LT992437.1	OW848999.1	*Klebsiella pneumoniae*	40,577	100	99.98	0	2016	Spain
LT992437.1	KY913901.1	*Klebsiella oxytoca*	40,275	100	99.98	0	–	China
LT992437.1	CP032895.1	*Enterobacter kobei*	43,125	100	99.97	0	2017	China
LT992437.1	OW849539.1	*Klebsiella pneumoniae*	40,359	100	99.95	0	2015	Spain
LT992437.1	CP080103.1	*Klebsiella quasipneumoniae*	40,407	100	99.93	0	2018	Argentina
LT992437.1	CP093216.1	*Escherichia coli*	43,534	100	99.75	0	2020/06/25	Croatia
LT992437.1	OW849084.1	*Citrobacter freundii*	40,203	100	99.74	0	2018	Spain
LT992437.1	OW969726.1	*Enterobacter cloacae*	40,408	99	99.97	0	2014	Spain
LT992437.1	OW848977.1	*Enterobacter cloacae*	40,289	99	99.97	0	2016	Spain
LT992437.1	OW849381.1	*Escherichia coli*	40,408	99	99.97	0	2016	Spain
LT992437.1	OW849079.1	*Enterobacter cloacae*	40,646	99	99.97	0	2016	Spain
LT992437.1	CP182930.1	*Citrobacter freundii*	46,509	99	99.62	0	2022	China
LT992437.1	MN539620.1	*Citrobacter sp.*	40,013	98	99.99	0	–	China
LT992437.1	OW967267.1	*Citrobacter freundii*	40,836	98	99.99	0	2018	Spain
LT992437.1	OW969792.1	*Klebsiella pneumoniae*	39,797	98	99.98	0	2014	Spain
LT992437.1	OW848983.1	*Escherichia coli*	39,780	98	99.98	0	2016	Spain
LT992437.1	CP040685.1	*Pseudomonas aeruginosa*	40,180	98	99.50	0	2017/09/22	China
LT992437.1	MH909348.1	*Klebsiella pneumoniae*	42,055	96	100.00	0	2013	China
LT992437.1	OW969822.1	*Klebsiella pneumoniae*	43,808	96	100.00	0	2014	Spain
LT992437.1	OW969816.1	*Klebsiella pneumoniae*	39,199	96	100.00	0	2012	Spain

Continued

Query	Target	Target species	Target length	Query cover (%)	Identities (%)	E value	Collection date	Geographic location
LT992437.1	OW969809.1	*Klebsiella pneumoniae*	39,216	96	100.00	0	2012	Spain
LT992437.1	OW969787.1	*Enterobacter cloacae*	39,386	96	100.00	0	2012	Spain
LT992437.1	CP028566.1	*Aeromonas hydrophila*	38,976	96	100.00	0	2015	China
LT992437.1	CP026224.1	*Aeromonas sp. ASNIH3*	39,148	96	100.00	0	2014	USA
LT992437.1	KR014106.1	*Aeromonas hydrophila*	44,451	96	100.00	0	–	China
LT992437.1	AP019194.1	*Aeromonas hydrophila*	39,071	96	100.00	0	2018/08	Japan
LT992437.1	OW969906.1	*Citrobacter freundii*	43,157	96	100.00	0	2015	Spain
LT992437.1	CP079843.1	*Escherichia coli*	41,744	96	100.00	0	2020/09	China
LT992437.1	AP022283.1	*Aeromonas veronii*	47,395	96	100.00	0	2019/02/05	Japan
LT992437.1	AP022253.1	*Aeromonas hydrophila*	39,071	96	100.00	0	2018/08/06	Japan
LT992437.1	MN477223.1	*Enterobacter cloacae*	39,013	96	99.99	0	–	China
LT992437.1	OW970313.1	*Klebsiella pneumoniae*	39,114	96	99.99	0	2013	Spain
LT992437.1	OW969914.1	*Klebsiella variicola*	39,199	96	99.99	0	2016	Spain
LT992437.1	OW969903.1	*Klebsiella pneumoniae*	39,388	96	99.99	0	2014	Spain
LT992437.1	OW969864.1	*Klebsiella pneumoniae*	39,148	96	99.99	0	2013	Spain
LT992437.1	OW969856.1	*Klebsiella pneumoniae*	39,199	96	99.99	0	2014	Spain
LT992437.1	OW969852.1	*Klebsiella pneumoniae*	39,216	96	99.99	0	2013	Spain
LT992437.1	OW969826.1	*Klebsiella pneumoniae*	39,182	96	99.99	0	2013	Spain
LT992437.1	OW969796.1	*Klebsiella pneumoniae*	39,182	96	99.99	0	2013	Spain
LT992437.1	MH624130.1	*Aeromonas taiwanensis*	53,205	96	99.99	0	–	China
LT992437.1	CP079826.1	*Aeromonas veronii*	51,662	96	99.99	0	2019/06	China
LT992437.1	MH909350.1	*Klebsiella pneumoniae*	39,014	96	99.98	0	2013	China
LT992437.1	CP018968.1	*Escherichia coli*	44,320	96	99.94	0	2011	Vietnam
LT992437.1	KU578314.1	*Pseudomonas aeruginosa*	38,939	96	99.91	0	–	China
LT992437.1	CP109826.1	*Serratia marcescens*	39,600	95	100.00	0	2021/10	China
LT992437.1	AP022277.1	*Enterobacter cloacae*	46,974	95	99.99	0	2019/02/05	Japan
LT992437.1	OW969689.1	*Citrobacter freundii*	38,347	94	100.00	0	2016	Spain
LT992437.1	OW848790.1	*Citrobacter freundii*	38,483	94	100.00	0	2018	Spain
LT992437.1	CP163081.1	*Citrobacter freundii*	45,124	94	99.99	0	2016/05	China
LT992437.1	AP022243.1	*Aeromonas caviae*	53,629	94	99.97	0	2018/08/06	Japan
LT992437.1	AP019197.1	*Aeromonas caviae*	53,629	94	99.97	0	2018/08	Japan
MH909337.1	CP064181.1	*Citrobacter amalonaticus*	52,790	100	100.00	0	2013/01/18	China
MH909337.1	MF344557.1	*Klebsiella pneumoniae*	56,893	100	100.00	0	–	China
MH909337.1	CP028486.1	*Escherichia coli*	52,864	100	100.00	0	2017/02/07	China
MH909337.1	KT989599.1	*Citrobacter freundii*	53,653	100	100.00	0	–	China
MH909337.1	CP098781.1	*Enterobacter hormaechei*	52,492	100	99.99	0	2017/03	China
MH909337.1	MH909334.1	*Klebsiella pneumoniae*	53,619	100	99.99	0	2011	China
MH909337.1	KU051709.1	*Escherichia coli*	51,600	100	99.98	0	–	China
MH909337.1	CP040895.1	*Leclercia adecarboxylata*	94,635	100	99.98	0	2018/11	China
MH909337.1	CP073923.1	*Klebsiella pneumoniae*	54,314	100	99.98	0	2015/12/23	China
MH909337.1	CP059714.1	*Enterobacter hormaechei*	52,787	100	99.98	0	2019/08/08	China
MH909337.1	KU862632.1	*Klebsiella pneumoniae*	51,591	100	99.97	0	–	–

Continued

Query	Target	Target species	Target length	Query cover (%)	Identities (%)	E value	Collection date	Geographic location
MH909337.1	KT982616.1	*Escherichia coli*	54,449	100	99.96	0	–	China
MH909337.1	KT982615.1	*Escherichia coli*	54,449	100	99.96	0	–	China
MH909337.1	KT989376.1	*Escherichia coli*	54,449	100	99.96	0	–	China
MH909337.1	KT982618.1	*Escherichia coli*	51,589	100	99.95	0	–	China
MH909337.1	KU886034.1	*Klebsiella pneumoniae*	51,599	100	99.93	0	–	China
MH909337.1	MK036890.1	*Klebsiella pneumoniae*	56,047	99	100.00	0	2009	China
MH909337.1	MH909339.1	*Klebsiella pneumoniae*	51,393	99	100.00	0	–	China
MH909337.1	CP102437.1	*Klebsiella pneumoniae*	163,393	99	100.00	0	2021/09/05	China
MH909337.1	KX711879.1	*Pseudomonas aeruginosa*	51,207	99	99.99	0	–	China
MH909337.1	CP052763.1	*Klebsiella pneumoniae*	52,578	99	99.99	0	2013/12/15	China
MH909337.1	MF072962.1	*Citrobacter freundii*	51,104	99	99.99	0	–	China
MH909337.1	KM977631.1	*Klebsiella pneumoniae*	50,742	99	99.99	0	–	China
MH909337.1	CP090265.1	*Escherichia coli*	52,202	99	99.99	0	2020	China
MH909337.1	CP050160.1	*Escherichia coli*	60,074	99	99.98	0	2016/09/28	China
MH909337.1	KU051708.1	*Klebsiella pneumoniae*	51,469	99	99.97	0	–	China
MH909337.1	MH909328.1	*Klebsiella pneumoniae*	50,480	99	99.97	0	–	China
MH909337.1	KU051707.1	*Escherichia coli*	51,362	99	99.96	0	–	China
MH909337.1	MH909336.1	*Klebsiella pneumoniae*	50,717	99	99.91	0	–	China
MH909337.1	ON882014.1	*Klebsiella pneumoniae*	52,398	99	99.79	0	–	China
MH909337.1	CP096924.1	*Enterobacter hormaechei*	55,933	98	100.00	0	2012	China
MH909337.1	KT989598.1	*Enterobacter cloacae*	54,669	98	99.96	0	–	–
MH909337.1	MH727565.1	*Citrobacter freundii*	51,795	98	99.92	0	2014/09/17	China
MH909337.1	KT982613.1	*Klebsiella pneumoniae*	50,979	98	99.91	0	–	China
MH909337.1	KU051710.1	*Citrobacter freundii*	50,546	97	100.00	0	–	China
MH909337.1	KY913900.1	*Klebsiella oxytoca*	61,680	97	99.93	0	–	China
MH909337.1	MW590809.1	*Klebsiella oxytoca*	62,892	96	100.00	0	–	–
MH909337.1	CP050159.1	*Enterobacter cloacae*	56,780	96	99.99	0	2014/06/03	China
MH909337.1	CP090255.1	*Escherichia coli*	49,457	96	99.98	0	2018	China
MH909337.1	CP092465.1	*Citrobacter freundii*	59,165	94	100.00	0	2021/09/27	China
MH909337.1	CP093156.1	*Enterobacter asburiae*	63,489	94	100.00	0	2019/06/19	China
MH909337.1	CP077825.1	*Klebsiella pneumoniae*	49,579	94	100.00	0	2018	Australia
MH909337.1	CP066846.1	*Escherichia coli*	60,935	94	100.00	0	2020/06	China
MH909337.1	CP098488.1	*Enterobacter hormaechei*	57,389	94	100.00	0	2019	China
MH909337.1	KM660724.1	*Morganella morganii*	57,797	94	100.00	0	–	USAn
MH909337.1	CP046118.1	*Enterobacter cloacae*	62,663	94	100.00	0	2017/03/29	China
MH909337.1	CP025965.2	*Klebsiella pneumoniae*	59,730	94	99.98	0	2017	China
MH909337.1	CP050859.2	*Klebsiella pneumoniae*	59,764	94	99.97	0	2016	China
MH909337.1	CP091489.1	*Enterobacter cloacae*	114,676	94	99.95	0	2020/12/13	China
MH909337.1	MW574949.1	*Escherichia coli*	67,069	93	99.99	0	–	Sweden
MH909337.1	MW574945.1	*Escherichia coli*	59,328	93	99.99	0	–	Sweden
MH909337.1	MW574936.1	*Escherichia coli*	67,066	93	99.99	0	–	Sweden
MH909337.1	CP096922.1	*Citrobacter freundii*	62,214	92	99.98	0	2014	China

Continued

Query	Target	Target species	Target length	Query cover (%)	Identities (%)	E value	Collection date	Geographic location
MH909337.1	LC663729.1	*uncultured bacterium*	67,562	91	99.99	0	–	–
MH909337.1	KJ933392.1	*Escherichia coli*	72,800	91	99.99	0	–	USA
MH909337.1	OP378618.1	*Escherichia coli*	205,325	91	99.98	0	–	–

Note: "–" means data not available.
Abbreviation: NCBI=National Center for Biotechnology Information.

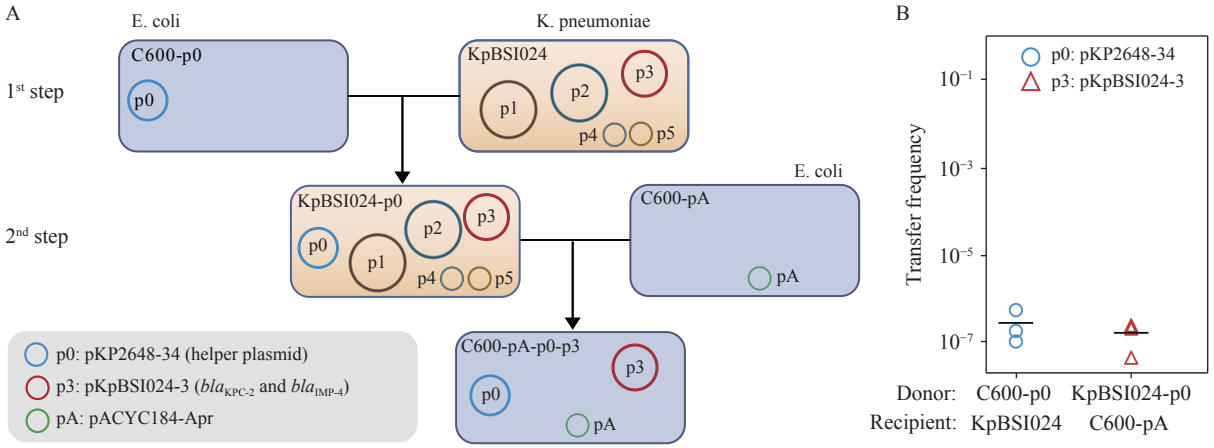

SUPPLEMENTARY FIGURE S1. Transfer of the mobilizable plasmid pKpBSI024-3 (p3), co-harboring *bla*KPC-2 and *bla*IMP-4, facilitated by the conjugative plasmid pKP2648-34 (p0). (A) Schematic representation of the two-step conjugation assay. In the first step, the helper plasmid pKP2648-34 (p0) was transferred from donor *E. coli* C600-p0 to the recipient CRKP *K. pneumoniae* KpBSI024. In the second step, pKpBSI024-3 (p3) was transferred into *E. coli* C600-pA with the assistance of pKP2648-34 (p0); (B) Transfer frequencies of the mobilizable plasmid pKpBSI024-3 (p3) and the conjugative plasmid pKP2648-34 (p0). Donor strains included *E. coli* C600-p0 and *K. pneumoniae* KpBSI024-p0, while recipient strains were *K. pneumoniae* KpBSI024 and *E. coli* C600-pA.
Abbreviation: CRKP=carbapenem-resistant *Klebsiella pneumoniae*; *E.coli=Escherichia coli*.

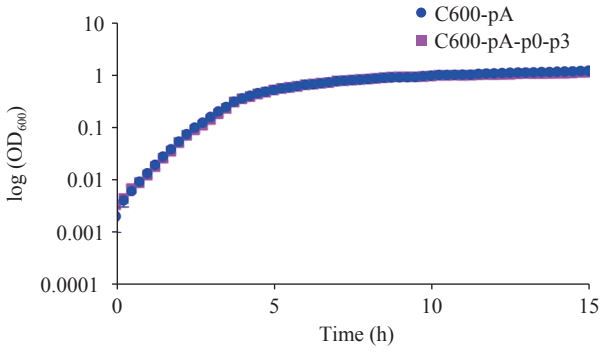

SUPPLEMENTARY FIGURE S2. Growth curves of *E. coli* C600-pA and its transconjugant *E. coli* C600-pA-p0-p3.

number of recipient cells. All conjugation assays were performed in triplicate.

Bacterial Growth Curve Analysis

To assess growth, overnight cultures of recipient strains and corresponding transconjugants were diluted 1:100 into fresh LB medium, incubated at 37 °C, and shaken at 220 rpm. To generate growth curves, OD_{600} readings were taken every 15 minutes using a spectrophotometer, with three technical replicates for each strain.

REFERENCES

1. Chen SF. Ultrafast one-pass FASTQ data preprocessing, quality control, and deduplication using fastp. iMeta 2023;2:e107. http://dx.doi.org/10.1002/imt2.107. https://doi.org/10.1002/imt2.107.
2. Wick RR, Judd LM, Gorrie CL, Holt KE. Unicycler: resolving bacterial genome assemblies from short and long sequencing reads. PLoS Comput Biol 2017;13(6):e1005595. https://doi.org/10.1371/journal.pcbi.1005595.
3. Seemann T. Prokka: rapid prokaryotic genome annotation. Bioinformatics 2014;30(14):2068 – 9. https://doi.org/10.1093/bioinformatics/btu153.
4. Wang M, Goh YX, Tai C, Wang H, Deng ZX, Ou HY. VRprofile2: detection of antibiotic resistance-associated mobilome in bacterial pathogens. Nucleic Acids Res 2022;50(W1):W768 – 73. https://doi.org/10.1093/nar/gkac321.
5. Zankari E, Hasman H, Cosentino S, Vestergaard M, Rasmussen S, Lund O, et al. Identification of acquired antimicrobial resistance genes. J Antimicrob Chemother 2012;67(11):2640 – 4. https://doi.org/10.1093/jac/dks261.
6. Carattoli A, Zankari E, García-Fernández A, Voldby Larsen M, Lund O, Villa L, et al. *In silico* detection and typing of plasmids using PlasmidFinder and plasmid multilocus sequence typing. Antimicrob Agents Chemother 2014;58(7):3895 – 903. https://doi.org/10.1128/AAC.02412-14.
7. Jolley KA, Bray JE, Maiden MCJ. Open-access bacterial population genomics: BIGSdb software, the PubMLST. org website and their applications. Wellcome Open Res 2018;3:124. https://doi.org/10.12688/wellcomeopenres.14826.1.
8. Alikhan NF, Petty NK, Ben Zakour NL, Beatson SA. BLAST Ring Image Generator (BRIG): simple prokaryote genome comparisons. BMC Genomics 2011;12:402. https://doi.org/10.1186/1471-2164-12-402.
9. Sullivan MJ, Petty NK, Beatson SA. Easyfig: a genome comparison visualizer. Bioinformatics 2011;27(7):1009 – 10. https://doi.org/10.1093/bioinformatics/btr039.
10. CLSI. CLSI M100 Performance standards for antimicrobial susceptibility testing. Clinical and Laboratory Standards Institute, 2025.
11. Zhang JF, Xu YP, Wang M, Li XB, Liu ZY, Kuang D, et al. Mobilizable plasmids drive the spread of antimicrobial resistance genes and virulence genes in *Klebsiella pneumoniae*. Genome Med 2023;15(1):106. https://doi.org/10.1186/s13073-023-01260-w.
12. Wang XL, Tang B, Liu GT, Wang M, Sun JY, Tan RM, et al. Transmission of nonconjugative virulence or resistance plasmids mediated by a self-transferable IncN3 plasmid from carbapenem-resistant *Klebsiella pneumoniae*. Microbiol Spectr 2022;10(4):e0136422. https://doi.org/10.1128/spectrum.01364-22.
13. Bartolomé B, Jubete Y, Martínez E, de la Cruz F. Construction and properties of a family of pACYC184-derived cloning vectors compatible with pBR322 and its derivatives. Gene 1991;102(1):75 – 8. https://doi.org/10.1016/0378-1119(91)90541-I.

Preplanned Studies

Genomic Insights into Genetic Characteristics of *Chromobacterium haemolyticum* — China, 2023

Bei Wei[1,&]; Yuhang Pei[2,&]; Yanan Wang[2,3,4,5,#]; Xuebin Xu[6,#]

Summary

What is already known about this topic?

Chromobacterium haemolyticum (*C. haemolyticum*) is an emerging multidrug-resistant and potentially extensively drug-resistant pathogen capable of causing invasive, lethal infections in humans. Conventional biochemical and mass spectrometry identification methods used in clinical laboratories cannot reliably distinguish it from *C. violaceum*.

What is added by this report?

This study provides the first report characterizing the genomic features of *C. haemolyticum* isolated from a young patient in China and reveals the evolutionary patterns of global *C. haemolyticum* isolates.

What are the implications for public health practice?

This research highlights the advantages of whole-genome sequencing for accurate differentiation of *Chromobacterium* species, raises public awareness about this uncommon pathogen, and provides scientific foundations for improved detection and prevention strategies.

ABSTRACT

Introduction: *Chromobacterium haemolyticum* (*C. haemolyticum*) can cause invasive infections in humans. This study aims to reveal the genomic characteristics of *C. haemolyticum* and provide guidance for clinical diagnosis, treatment, prevention, and control.

Methods: Species identification was performed through isolation culture and matrix-assisted laser desorption ionization time-of-flight mass spectrometry. Antibiotic susceptibility testing determined resistance phenotypes. High-throughput sequencing and bioinformatics methods were used to predict antibiotic resistance genes and virulence genes and to analyze the evolutionary characteristics of global *C. hemolyticus* genomes.

Results: In this study, a *C. haemolyticum* strain was isolated from the bronchoalveolar lavage fluid of a patient in Guangxi Zhuang Autonomous Region, China. The isolate was sensitive to chloramphenicol, macrolides, and trimethoprim, while resistant to beta-lactams. Comparative genomics analysis revealed that most global strains carry carbapenemase-encoding genes. Phylogenetic analysis showed that the strain from this patient was closely related to a pond-derived *C. haemolyticum* isolate from Yangzhou, China.

Conclusions: This study uncovered the genetic characteristics of *C. haemolyticum* from various sources worldwide, including antibiotic resistance and virulence factors, providing an important reference for clinical treatment.

The genus *Chromobacterium* belongs to the family *Neisseriaceae* and comprises 19 species (*1*). *Chromobacterium violaceum* (*C. violaceum*) is a zoonotic pathogen found in tropical and subtropical regions that can cause severe sepsis with high mortality rates in humans (*2*). Since the first report of *C. haemolyticum* in 2008 (*3*), most invasive infection cases (e.g., pneumonia and bacteremia) have been associated with exposure to water bodies (*4*). However, genomic data on *C. haemolyticum* remains insufficient worldwide.

Here, we report the first case of pulmonary infection caused by *Chromobacterium* spp. in Guigang City, Guangxi Zhuang Autonomous Region, China. On the evening of November 4, 2023, an 18-year-old patient was admitted to the Qintang District People's Hospital following a traffic accident in Guigang City. The patient subsequently developed pneumonia and a *Chromobacterium* spp. strain was isolated from bronchoalveolar lavage fluid. After combined treatment with cefoperazone sodium/sulbactam sodium, meropenem, and levofloxacin, the patient recovered.

Antibiotic susceptibility testing (AST) was conducted according to the Clinical and Laboratory Standards Institute (CLSI) guidelines for non-*Enterobacteriaceae* bacteria to determine the minimum

inhibitory concentration (MIC) of the *C. haemolyticum* strain (*5*). The AST results are presented in Table 1. Overall, the strain demonstrated sensitivity to most antibiotics tested while exhibiting resistance to several beta-lactam and aminoglycoside antibiotics (Table 1 and Supplementary Table S1, available at https://weekly.chinacdc.cn/).

The isolate was initially identified as *C. violaceum* using blood agar culture, biochemical experiments, and matrix-assisted laser desorption ionization time-of-flight mass spectrometry (MALDI-TOF MS) (model: VITEK MS, version: VITEK MS V3.0, BioMérieux, France). Due to similar cultural characteristics between the two species, *C. haemolyticum* is frequently misidentified as *C. violaceum* (*6*). Definitive identification as *C. haemolyticum* was subsequently achieved (Supplementary Table S2, available at https://weekly.chinacdc.cn/) using MetaphlAn4 with database version mpa_vOct22_CHOCOPhlAnSGB_202212 (*7*).

We downloaded 19 publicly available genomes of *C. haemolyticum* from the National Center for Biotechnology Information (NCBI) to characterize genomic features. After excluding two low-quality genomes (GCF_000285415.1 and GCF_003332145.1), the remaining 17 genomic datasets were used for subsequent analysis (Supplementary Table S3, available at https://weekly.chinacdc.cn/). We detected 12 antibiotic resistance genes (ARGs) classified into 7 categories (Supplementary Tables S1 and Supplementary Table S4, available at https://weekly.chinacdc.cn/). The predominant ARGs were *rpsJ* and four mutated genes: *gidB*, *MurA*, *folP*, and *gyrA*. Additionally, carbapenemase-encoding genes, including $bla_{\text{CRH-1}}$, $bla_{\text{CRH-2}}$, and $bla_{\text{CRH-3}}$ were detected in 72.22% (13/18), 11.11% (2/18), and 16.67% (3/18) isolates, respectively. Moreover, we identified five types of multiple efflux pump systems-encoding genes (EmrAB-OMF, EmrAB-TolC, MdfA/CMr, MdtABC-TolC, and MacAB-TolC) that can reduce drug susceptibility.

We detected 9 virulence factors (VFs), with 33.33% (3/9) belonging to the type 3 secretion system (Supplementary Table S5, available at https://weekly.chinacdc.cn/). Among these VFs, *sicA*, *spaQ*, *spaT*, *fba*, *hfq*, and *recA* were present in all strains. To investigate potential drivers mediating ARGs and VFs transfer, we identified 59 intact prophages belonging to 19 types (Supplementary Table S6, available at https://weekly.chinacdc.cn/). The most prevalent prophage was *Mannhe_vB_MhM_3927AP2* (83.33%), followed by *Ralsto_RSA1* (33.33%), *Haemop_SuMu* (27.78%), and *Burkho_phiE125* (27.78%).

To explore the population evolution of *C. haemolyticum*, we analyzed 18 public *C. haemolyticum* genomes and 2 *C. violaceum* genomes (*8*). The phylogenetic tree revealed two distinct lineages corresponding to the two different species, spanning

TABLE 1. Results of antibiotic susceptibility testing.

Antibiotic	MIC (μg/mL)	Interpretation
Imipenem	4	S
Meropenem	≤1	S
Piperacillin	≥128	R
Piperacillin/tazobactam	≤4/4	S
Cefepime	≤2	S
Ceftazidime	≤2	S
Minocycline	≤4	S
Cefoperazone/Sulbactam	≤8/4	S
Sulfamethoxazole/Trimethoprim	≤1/19	S
Gentamicin	≤2	S
Amikacin	32	I
Levofloxacin	≤1	S
Ciprofloxacin	≤0.5	S
Chloramphenicol	≤8	S
Aztreonam	≤2	S

Note: S indicates sensitivity, R indicates resistant, and I indicates intermediate.

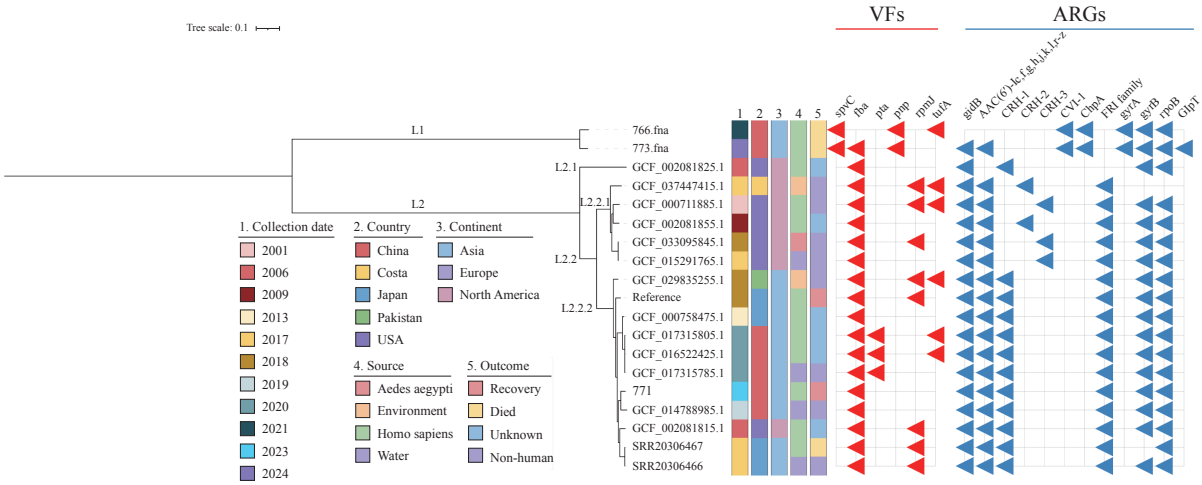

FIGURE 1. Phylogenetic analysis of 19 *C. haemolyticum* genomes.
Note: Phylogenetic tree-built details and analysis are described in the text. Collection date, country, source, continent, and outcome are labeled with different colors. The red and blue triangles represent the existence of VFs and ARGs, respectively.
Abbreviation: VFs=virulence factors; ARGs=antibiotic resistance genes.

five countries and four diverse sources (human, water, environment, and *Aedes aegypti*) (Figure 1). Lineage one (L1) consisted of 2 *C. violaceum* strains from China, while lineage two (L2) comprised global *C. haemolyticum* strains. The isolate from the patient in this study showed a close genetic relationship with a pond-source *C. haemolyticum* strain from Yangzhou, China. Both isolates exhibited fewer virulence factors, with 6 VFs each.

DISCUSSION

Advances in whole-genome sequencing (WGS) enable rapid and accurate species identification and tracking of potential factors and evolutionary patterns of existing and emerging antibiotic resistance (AMR) and virulence factors in bacteria that inhabit organisms and the environment (*8–12*) Using WGS, we successfully distinguished the genetic differences between the *C. haemolyticum* strain in our study and *C. violaceum*, confirming the identify of our isolate as *C. haemolyticum* (Supplementary Table S6, available at https://weekly.chinacdc.cn/).

Carbapenem-resistant gram-negative bacteria pose a significant health burden (*13–15*). Carbapenemase-encoding genes naturally exist in the chromosomes of *Chromobacterium* species (*16*). We detected $bla_{\text{CRH-1}}$ in 13 strains of *C. haemolyticum*, while $bla_{\text{CRH-2}}$ and $bla_{\text{CRH-3}}$ were detected in 2 and 3 strains, respectively. Additionally, we identified mutated fluoroquinolone resistance genes (*gyrA* and *gyrB*) and the tetracycline resistance gene *rpsJ*. However, the *C. haemolyticum* isolate from our patient remained sensitive to ciprofloxacin, nalidixic acid, meropenem, tetracycline, and tigecycline, suggesting these ARGs may not be expressed (*12*).

In summary, this is the first report characterizing the genome of *C. haemolyticum* causing human pulmonary infection in China. We found that the strain isolated from the recovered patient carried fewer virulence factors and shared a close genetic relationship with a water isolate from Yangzhou, China. Due to the limited number of available genomes, which may underestimate the global transmission risk of carbapenem-resistant *C. haemolyticum*, increased genomic surveillance is needed to better understand its spread and evolutionary trajectory. Our findings enhance awareness of this uncommon species and provide a scientific basis for the prevention and treatment of infections caused by *C. haemolyticum* in humans, food animals, and ornamental animals in the future.

Conflicts of interest: No conflicts of interest.

Acknowledgements: The Veterinary Big Data and Bioinformatics Center, Henan Agricultural University for their support and assistance.

Funding: Supported by grants from the National Key Research and Development Program of China (2023YFC2307101), the Young TopNotch Talents Foundation of Henan Agricultural University (30501278), and Project for Young Scientist of the Joint Funds of Science and Technology Research and Development Plan of Henan Province, China (235200810058).

doi: 10.46234/ccdcw2025.148

[#] Corresponding authors: Xuebin Xu, xuxuebin@scdc.sh.cn; Yanan Wang, wangyanan1001@henau.edu.cn.

[1] Department of Laboratory Medicine, Qintang District People's Hospital, Guigang City, Guangxi Zhuang Autonomous Region, China; [2] International Joint Research Center of National Animal Immunology, College of Veterinary Medicine, Henan Agricultural University, Zhengzhou City, Henan Province, China; [3] CAS Key Laboratory of Pathogen Microbiology and Immunology, Institute of Microbiology, Chinese Academy of Sciences, Beijing, China; [4] Longhu Laboratory of Advanced Immunology, Zhengzhou City, Henan Province, China; [5] Henan Academy of Innovations in Medical Science, Zhengzhou City, Henan Province, China; [6] Division of Pathogen Testing and Analysis, Shanghai Municipal Center for Disease Control and Prevention, Shanghai, China.
[&] Joint first authors.

Submitted: April 03, 2025
Accepted: June 19, 2025
Issued: August 08, 2025

REFERENCES

1. DSMZ-Deutsche sammlung von mikroorganismen und zellkulturen. 2024. https://www.bionity.com/de/lexikon/Deutsche_Sammlung_von_Mikroorganismen_und_Zellkulturen.html.
2. Alisjahbana B, Debora J, Susandi E, Darmawan G. *Chromobacterium violaceum*: a review of an unexpected scourge. Int J Gen Med 2021;14:3259 – 70. https://doi.org/10.2147/IJGM.S272193.
3. Han XY, Han FS, Segal J. *Chromobacterium haemolyticum* sp. nov., a strongly haemolytic species. Int J Syst Evol Microbiol 2008;58(Pt 6):1398-403. http://dx.doi.org/10.1099/ijs.0.64681-0.
4. Iwamoto K, Yamamoto M, Yamamoto A, Sai T, Mukai T, Miura N, et al. Meningitis caused by *Chromobacterium haemolyticum* suspected to be derived from a canal in Japan: a case report. J Med Case Rep 2023;17(1):171. https://doi.org/10.1186/s13256-023-03913-1.
5. CLSI. CLSI M100 Performance standards for antimicrobial susceptibility testing. 33rd ed. CLSI, 2023. https://clsi.org/about/news/clsi-publishes-m100-performance-standards-for-antimicrobial-susceptibility-testing-33rd-edition/.
6. Teixeira P, Tacão M, Baraúna RA, Silva A, Henriques I. Genomic analysis of *Chromobacterium haemolyticum*: insights into the species resistome, virulence determinants and genome plasticity. Mol Genet Genomics 2020;295(4):1001 – 12. https://doi.org/10.1007/s00438-020-01676-8.
7. Blanco-Míguez A, Beghini F, Cumbo F, Mciver LJ, Thompson KN, Zolfo M, et al. Extending and improving metagenomic taxonomic profiling with uncharacterized species using MetaPhlAn 4. Nat Biotech 2023;41(11):1633 – 44. https://doi.org/10.1038/s41587-023-01688-w.
8. Pei YH, Wei B, Huang HR, Wang YN, Xu XB. Global population structure and genomic insights into *Chromobacterium violaceum* of human invasive lethal infection and non-human origins. J Infect 2024;89(6):106332. https://doi.org/10.1016/j.jinf.2024.106332.
9. Wang YN, Liu Y, Lyu N, Li ZY, Ma SF, Cao DM, et al. The temporal dynamics of antimicrobial-resistant *Salmonella enterica* and predominant serovars in China. Natl Sci Rev 2023;10(3):nwac269. https://doi.org/10.1093/nsr/nwac269.
10. Wang YN, Xu XB, Jia SL, Qu MQ, Pei YH, Qiu SF, et al. A global atlas and drivers of antimicrobial resistance in *Salmonella* during 1900-2023. Nat Commun 2025;16(1):4611. https://doi.org/10.1038/s41467-025-59758-3.
11. Wang YN, Xu XB, Zhu BL, Lyu N, Liu Y, Ma SF, et al. Genomic analysis of almost 8,000 *Salmonella* genomes reveals drivers and landscape of antimicrobial resistance in China. Microbiol Spectr 2023;11(6):e0208023. https://doi.org/10.1128/spectrum.02080-23.
12. Lv PP, Pei YH, Jiang Y, Wang Q, Liu Y, Qu MQ, et al. Genomic insights into antibiotic-resistant non-typhoidal *Salmonella* isolates from outpatients in Minhang District in Shanghai. Commun Med 2025;5(1):228. https://doi.org/10.1038/s43856-025-00950-3.
13. World Health Organization. WHO bacterial priority pathogens list, 2024: bacterial pathogens of public health importance to guide research, development and strategies to prevent and control antimicrobial resistance. Geneva: World Health Organization; 2024. https://www.who.int/publications/i/item/9789240093461.
14. Ma YY, Chen P, Mo Y, Xiao YH. WHO revised bacterial priority pathogens list to encourage global actions to combat AMR. hLife 2024;2(12):607 – 10. https://doi.org/10.1016/j.hlife.2024.10.003.
15. Xiao YH, Nishijima T. Status and challenges of global antimicrobial resistance control: a dialogue between Professors Yonghong Xiao and Takeshi Nishijima. hLife 2024;2(2):47 – 9. https://doi.org/10.1016/j.hlife.2023.11.004.
16. Gudeta DD, Bortolaia V, Jayol A, Poirel L, Nordmann P, Guardabassi L. *Chromobacterium* spp. harbour Ambler class A β-lactamases showing high identity with KPC. J Antimicrob Chemother 2016;71(6):1493 – 6. https://doi.org/10.1093/jac/dkw020.

Preplanned Studies

Genomic Characteristics and Antibiotic Resistance Evolution of Vibrio cholerae O139 — Anhui Province, China, 2013–2024

Weiwei Li[1]; Yong Sun[1]; Tai Ma[1]; Wanhang Lu[1]; Nan Sa[1]; Lei Gong[1]; Xinxin Wang[1]; Jiaming Tian[1]; Yongkang Xiao[1]; Liangliang Jiang[3]; Xiangying Wang[4]; Ge Bu[5]; Guozhou Liu[6]; Xiaoxue Yang[1]; Zhuhui Zhang[1]; Wenchang Li[1]; Jinbao Huang[2,#]; Zhiguo Cao[1,#]

Summary

What is already known about this topic?

Cholera, a severe diarrheal disease caused by *Vibrio cholerae*, remains a major global public health concern. In 2023, the World Health Organization reported 535,321 cholera cases and 4,007 deaths in 45 countries. Sporadic cases and epidemic outbreaks of the cholera serogroup O139 have been documented in various Chinese provinces since 1993.

What is added by this report?

This study analyzed the genomic features and antibiotic resistance patterns of 34 *Vibrio cholerae* O139 strains collected in Anhui Province between 2013 and 2024. The genetic sequences exhibited closer relationships to strains isolated from China than to those from India and Bangladesh, primarily forming two clusters. These strains contain multiple virulence factors, antimicrobial resistance (AMR) genes, and mobile genetic elements (MGEs). Notably, over 50% of the strains lacked the *vgr*G-2 gene in the type 6 secretion system (T6SS). Additionally, an increasing trend in azithromycin resistance was observed, whereas trimethoprim-sulfamethoxazole resistance showed a decreasing trend.

What are the implications for public health practice?

Vibrio cholerae O139 in Anhui Province displayed genomic diversity indicative of domestic origin rather than cross-border transmission. While their pathogenicity is limited, these strains demonstrate robust colonization capabilities and the potential to disseminate AMR genes. The shift in AMR profiles driven by the clinical use of azithromycin poses an ongoing transmission risk for O139 strains and may foster the further emergence of AMR in the region.

Abstract

Objective: Recent cholera outbreaks in Anhui Province have been linked to *Vibrio cholerae* O139, but information on these strains is limited. We established the first genomic dataset of local O139 strains to analyze the genomic characteristics and evolution of antibiotic resistance.

Methods: Thirty-four *Vibrio cholerae* O139 isolates from Anhui (2013–2024) were sequenced using next-generation sequencing. Genes for virulence, antimicrobial resistance, pathogenicity islands, and mobile genetic elements were predicted using ABRicate and other online tools. To construct a phylogenetic tree, 124 publicly available O139 genomes were included in the single-nucleotide polymorphism analysis alongside the study isolates.

Results: Strains formed two clusters that were genetically closer to China isolates than with those from Bangladesh and India. All strains harbored *ctxA* and *ctxB*, with partial deletions in virulence genes and pathogenicity islands; over 50% lacked *vgrG-2* in the T6SS. Strains from 2022–2024 exhibited higher azithromycin but lower trimethoprim-sulfamethoxazole resistance than those collected during 2013–2017.

Conclusion: *Vibrio cholerae* O139 in Anhui are endemic to China, with limited virulence but strong colonization abilities. The increased azithromycin resistance rate may be driven by its clinical antimicrobial usage, suggesting its potential for continued antibiotic resistance evolution.

Vibrio cholerae serogroups O1 and O139 are known to cause cholera pandemics. Since 1817, seven global cholera pandemics have occurred, with the ongoing seventh pandemic beginning in 1961 (*1*). The global spread of O1 El Tor biotype has replaced the classical biotype as the cause of the current pandemic. In 1992–1993, the O139 serogroup first emerged, triggering outbreaks in India and Bangladesh, and was

genetically derived from El Tor biotype strains (*2*–*4*). Unlike its widespread epidemics in Bangladesh and India, the O139 serogroup caused limited foodborne outbreaks in China (*5*). Nevertheless, recent studies indicate that O139 continues to cause sporadic outbreaks in this region. The first O139 cholera outbreak in China occurred in Xinjiang in 1993, with subsequent case reports from other provinces (*6*). Anhui Province detected its first O139 serogroup outbreak in 1996 (*7*). Although sporadic cases have persisted in the region, the genomic characteristics of these strains and their evolutionary relationships with isolates from other regions of China and Asia remain unclear. Antibiotics such as azithromycin (AZM), ciprofloxacin (CIP), and doxycycline are recommended for the clinical management of cholera (*4*). However, the recent emergence of antimicrobial resistance (AMR) in *Vibrio cholerae* has become an increasing concern. A study in China reported consistently high levels of resistance to streptomycin, trimethoprim-sulfamethoxazole (SXT), erythromycin, and polymyxin B among O139 serogroups from 1993 to 2009 (*5*). Since then, data on antibiotic resistance in these strains have been scarce.

Thus, to explore the genetic and antimicrobial features of *Vibrio cholerae* O139 in the Anhui Province, we analyzed 34 strains collected by the Anhui Provincial Center for Disease Control and Prevention from 2013 to 2024, sequenced their whole genomes, and assessed their drug resistance profiles.

Whole-genome sequencing was performed using MGISEQ2000 or Illumina NovaSeq platforms. Single-nucleotide polymorphisms (SNPs) were identified using Snippy (version 4.6.0; The University of Melbourne) and recombinant SNPs were removed using Gubbins (version 2.4.1; The Wellcome Trust Sanger Institute). The reference genome sequence was obtained from Bangladesh (GCF_900324445.1) (*8*). A maximum-likelihood phylogenetic tree was constructed using IQ-TREE (version 2.2.6; Australian National University). The AMR, virulence, and plasmid genes were predicted using ABRicate (version 1.0.1; The University of Melbourne) in the CARD, VFDB, and PlasmidFinder databases, respectively. Cholerae Finder v1.0 (https://cge.food.dtu.dk/services/CholeraeFinder/) was used to analyze the seventh pandemic islands (VSP-1 and VSP-2) and mobile genetic element (MGE) genes (*intI* 1 and *int*SXT). Antimicrobial susceptibility testing using broth microdilution for ampicillin (AMP), ampicillin sulbactam (AMS), ceftazidime (CAZ), cefotaxime (CTX), chloramphenicol (CHL), AZM, CIP, meropenem (MEM), amikacin (AMI), tetracycline (TET), and SXT was used to determine the minimum inhibitory concentration using a commercially prepared panel (Fosun Diagnostic, Shanghai, China). Results were interpreted according to the breakpoints defined by the Clinical and Laboratory Standards Institute. *Escherichia coli* ATCC25922 was used as the control.

Among the 34 strains, 33 were isolated from nine foodborne cholera outbreaks across six cities in Anhui Province, while one was identified through cholera surveillance in 2013. During the nine outbreaks, 28 cases were reported, including one in Jiangsu Province and another imported from Henan Province. Three outbreaks involved more than two cases; most individuals were asymptomatic. Epidemiological investigations revealed that six of the nine outbreaks were associated with banquets, and in four of these, turtles were the suspected food source. Twenty-seven strains were isolated from 26 cases. Three strains were isolated from turtle specimens, two of which were associated with outbreaks, and four strains were isolated from environmental samples, such as sewage, turtle cages, and closed stools, based on an epidemiological analysis (Table 1).

A total of 1,118 SNPs were identified across our isolates and 124 publicly available *Vibrio cholerae* O139 sequences from India, Bangladesh, and China. Of these, 870 SNPs were located on chromosome I and 248 on chromosome II. The phylogenetic tree divided the isolates into three lineages. All isolates from this study, along with 90 from Zhejiang, and 9 from Shanghai, were classified under lineage 3. Thirty-one isolates from this study were distributed across two clusters within lineage 3. Cluster 1 consisted of four isolates from a 2015 outbreak and was supported by eight SNPs. Cluster 2 consisted of 27 isolates from six outbreaks from 2022–2023, supported by 11 SNPs. One environmental isolate from the 2023 outbreak showed significant evolutionary divergence from its associated case isolate, differing by 181 SNPs. Three additional isolates were found outside of the two clusters (Figure 1).

All 34 isolates harbored *ctx*A and *ctx*B, whereas five lacked additional CTX phage genes. The majority also harbored additional toxin genes and various pilus-encoding genes, such as *pil*A and MSHA genes. Variable deletions were observed within the T6SS and pathogenicity islands, with *vgr*G-2 deleted in >50% of

TABLE 1. Epidemic information of the 34 *Vibrio cholerae* O139 isolates.

Strain	City	Isolation year	Isolation source	Clinical symptom	Outbreak No.	Suspected source	No. of cases
AH13HB006	Huaibei	2013	Turtle	–	–	–	–
AH15TC021	Chuzhou	2015	Anal swab	Asymptomatic carrier	1	Banquet/ Turtle	2*
AH15FY014	Fuyang	2015	Stool	Confirmed case	2	Banquet/ Turtle	1
AH15FY015	Fuyang	2015	Turtle	–	2		
AH15FY016	Fuyang	2015	Turtle cage	–	2		
AH15FY017	Fuyang	2015	Turtle cage	–	2		
AH17WXA018	Bozhou	2017	Stool	Confirmed case	3	Unknown	1†
AH22BZ152	Bozhou	2022	Stool	Confirmed case	4	Banquet/ Turtle	1§
AH22BZ153	Bozhou	2022	Stool	Confirmed case	4		
AH22BZ157-1	Bozhou	2022	Turtle	–	4		
AH22BZ154	Bozhou	2022	closestool	–	4		
AH22BB0202	Bengbu	2022	Anal swab	Confirmed case	5	Banquet/ Unknown	9¶
AH22BB0210	Bengbu	2022	Anal swab	Asymptomatic carrier	5		
AH22BB0209	Bengbu	2022	Anal swab	Asymptomatic carrier	5		
AH22BB0208	Bengbu	2022	Anal swab	Asymptomatic carrier	5		
AH22BB0207	Bengbu	2022	Anal swab	Asymptomatic carrier	5		
AH22BB0206	Bengbu	2022	Anal swab	Asymptomatic carrier	5		
AH22BB0201	Bengbu	2022	Anal swab	Confirmed case	5		
AH22BB0205	Bengbu	2022	Anal swab	Asymptomatic carrier	5		
AH23SZ0001	Suzhou	2023	Stool	Confirmed case	6	Unknown	1
AH23SZ0002	Suzhou	2023	Sewage	–	6		
AH23BZ791	Bozhou	2023	Stool	Confirmed case	7	Banquet/ Unknown	1
AH23MAS0424	Maanshan	2023	Anal swab	Asymptomatic carrier	8	Banquet/ Turtle	11
AH23MAS0427	Maanshan	2023	Anal swab	Asymptomatic carrier	8		
AH23MAS0426	Maanshan	2023	Anal swab	Asymptomatic carrier	8		
AH23MAS0425	Maanshan	2023	Anal swab	Asymptomatic carrier	8		
AH23MAS0423	Maanshan	2023	Anal swab	Asymptomatic carrier	8		
AH23MAS0422	Maanshan	2023	Anal swab	Asymptomatic carrier	8		
AH23MAS0421	Maanshan	2023	Anal swab	Confirmed case	8		
AH23MAS0420	Maanshan	2023	Anal swab	Asymptomatic carrier	8		
AH23MAS0419	Maanshan	2023	Anal swab	Asymptomatic carrier	8		
AH23MAS0418	Maanshan	2023	Stool	Asymptomatic carrier	8		
AH23MAS0417	Maanshan	2023	Stool	Confirmed case	8		
AH24BB0141	Bengbu	2024	Stool	Confirmed case	9	Shrimp	1

Note: *Two cases were associated with the same banquet in Anhui Province, and the other one was confirmed to have been found in Jiangsu Province.
† Imported case from Henan Province.
§ Two stool samples were collected from the same patient on different days.
¶ A total of 9 cases were associated with three separate banquets, and 8 of these cases were analyzed in this study.
"–" means not applicable.

the isolates (Figure 2A). Thirteen AMR genes were highly prevalent (>88%) among the study isolates, whereas *sul*1, *dfr*A18, and *qac*E delta1 were detected only in isolates collected before 2017. The genes *mph*E, *mph*F, and *msr*E were primarily found in Cluster 2, whereas *aph* (3')-Ia, *aad*A2, *dfr*A12, and *tet*D were mainly associated with Cluster 1 (Figure 2B). All isolates contained intSXT, with 32 isolates carrying the

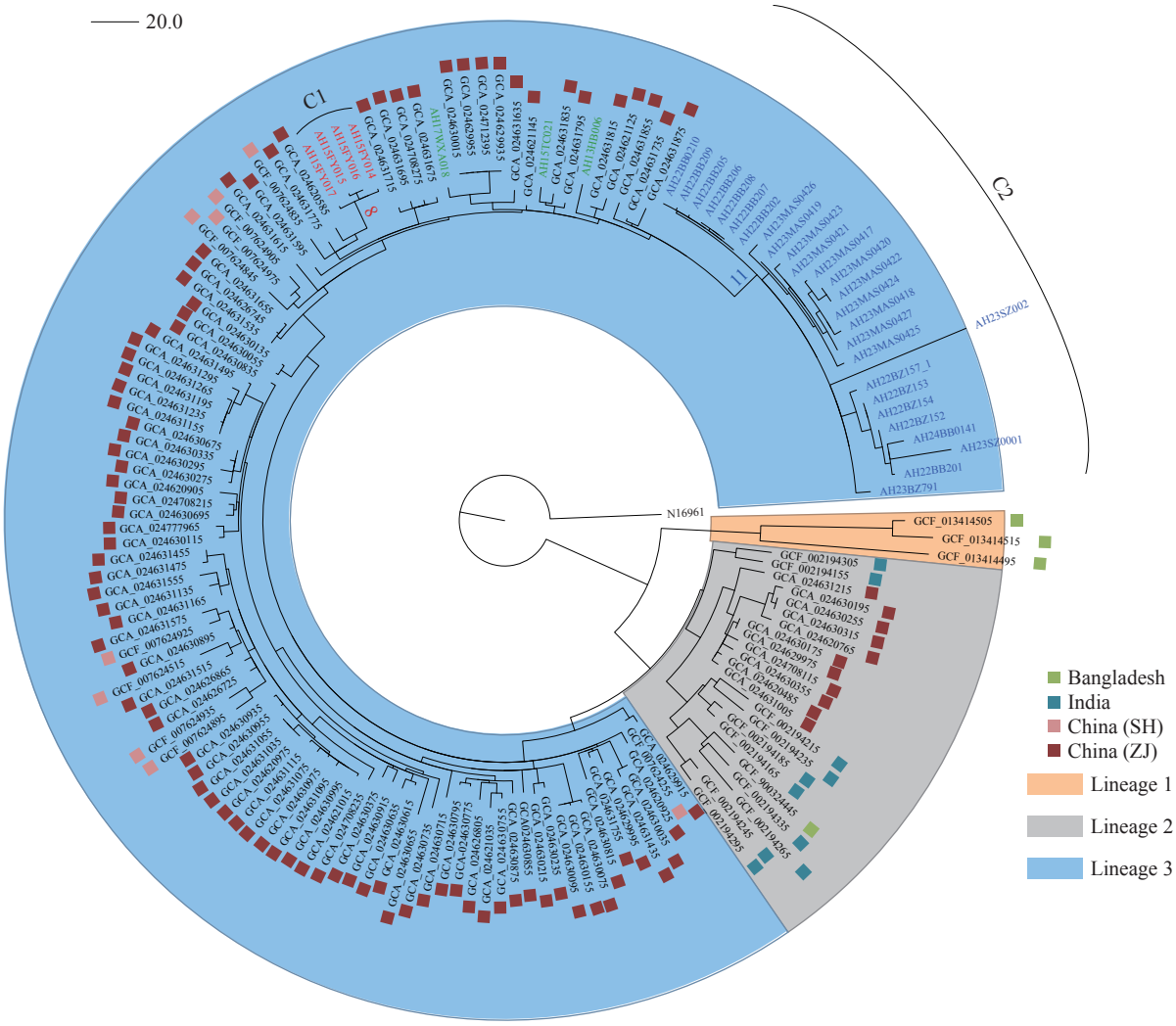

FIGURE 1. Maximum-likelihood phylogenetic tree of 158 *Vibrio cholerae* O139 isolates. The tree was rooted using the seventh pandemic O1 strain N16961 as the outgroup.
Note: The clusters C1 and C2 are depicted in red and blue, respectively. The number of SNPs supporting each cluster is marked on the respective branches. Three strains not belonging to either cluster are shown in green.
Abbreviation: SH=Shanghai; ZJ=Zhejiang.

IncA/C plasmid; however, only seven isolates collected from 2013–2017 contained *int*I 1 (Figure 2A).

All isolates were susceptible to MEM, CTX, CAZ, and AMI, with the majority being susceptible to AMP and AMS. Notably, high resistance rates to TET (91.18%) and AZM (76.55%) were observed, with AZM resistance particularly high among isolates collected during 2022–2024. All isolates collected during 2013–2017 exhibited 100% SXT resistance, whereas this was significantly lower (3.7%) among isolates collected between 2022 and 2024. Drug resistance patterns demonstrated a clear temporal trend, with TET-AZM resistance predominant in strains collected between 2022–2024 and TET-SXT resistance in those collected during 2013–2017 (Table 2).

DISCUSSION

In recent decades, foodborne outbreaks caused by *Vibrio cholerae* O139 with soft-shelled turtles as vectors have been frequently reported in China (*9*). This study established the first provincial-level genomic surveillance dataset for this pathogen in Anhui, addressing the critical data gap. From 2013 to 2024, all cholera cases in Anhui Province were attributed to the serogroup O139. Group dining and human mobility were identified as the key outbreak drivers, with phylogenetic analysis implicating turtles as transmission vehicles. The isolates showed closer

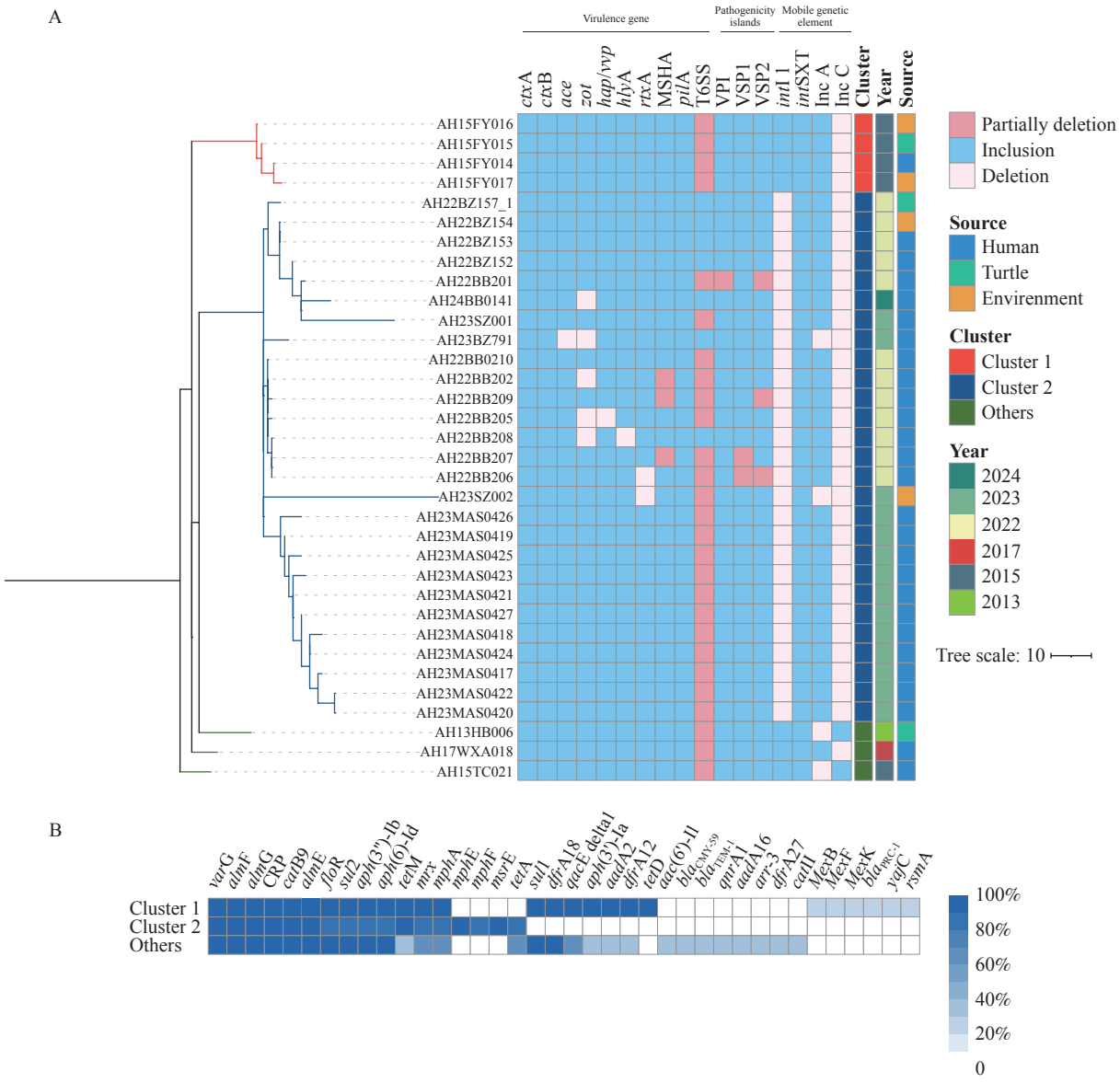

FIGURE 2. Genomic features of the 34 *Vibrio cholerae* O139 isolates. (A) Virulence genes, pathogenicity islands, and mobile genetic elements. (B) Distribution of antibiotic resistance genes across the different clusters.
Note: For (A), MSHA gene cluster includes *msh*HIJKLMNEGF and *msh*BACD. Both T6SS and VPI comprise 19 genes, as previously described (11). For (B), 'Others' represents three isolates that fall outside the two main clusters.
Abbreviation: MSHA=maltose-sensitive haemagglutinin.

genetic clustering with the Zhejiang and Shanghai strains than with other Asian strains, suggesting domestic circulation rather than cross-border transmission. Two temporally segregated clusters were identified within the Anhui isolates, demonstrating the ongoing evolution of *Vibrio cholerae* O139 in China. This pattern differs from three genetically distinct but temporally overlapping O139 clades that emerged in India and spread across South Asia between 1992 and 2015 (*10*).

Most isolates harbored multiple virulence genes but exhibited more deletions than Zhejiang O139 isolates (*11*) and those from other Asian countries (*10*), potentially affecting virulence. T6SS plays a crucial role in host-pathogen interactions via translocation. Deletion of *vgr*G-2 or both *vgr*G1 and *vgr*G3 severely impairs T6SS secretion in *Vibrio cholerae* (*12*). Thus, the absence of *vgr*G-2 in the study isolates might impair T6SS function, potentially explaining the limited cases and asymptomatic infections in Anhui Province. However, high prevalence of MSHA genes may enhance their environmental viability, particularly on the surface of turtles, where MSHA is essential for colonization (*9*).

TABLE 2. Antibiotic susceptibility patterns of the 34 *Vibrio cholerae* O139 isolates.

Antibiotic	2013–2017 (*n*=7)			2022–2024 (*n*=27)		
	S (%)	I (%)	R (%)	S (%)	I (%)	R (%)
CHL	4 (57.1)	2 (28.6)	1 (14.3)	10 (37.0)	17 (63.0)	0
SXT	0	0	7 (100)	26 (96.3)	0	1 (3.7)
MEM	7 (100)	0	0	27 (100)	0	0
CTX	7 (100)	0	0	27 (100)	0	0
CTZ	7 (100)	0	0	27 (100)	0	0
TET	2 (28.6)	1 (14.3)	4 (57.1)	0	0	27 (100)
CIP	6 (85.7)	1 (14.3)	0	27 (100)	0	0
AZM	7 (100)	0	0	1 (3.7)	0	26 (96.3)
AMI	7 (100)	0	0	27 (100)	0	0
AMP	6 (85.7)	0	1 (14.3)	27 (100)	0	0
AMS	6 (85.7)	0	1 (14.3)	27 (100)	0	0

Abbreviation: AMP=ampicillin; AMS=ampicillin sulbactam; CAZ=ceftazidime; CTX=cefotaxime; CHL=chloramphenicol; AZM=azithromycin; CIP=ciprofloxacin; MEM=meropenem; AMI=amikacin; TET=tetracycline; SXT=trimethoprim-sulfamethoxazole; S=susceptible; I=intermediate; R=resistant.

In China, the resistance rates to TET, CHL, AZM, and AMP in toxigenic O139 strains from 1993 to 2009 varied over time. Notably, TET resistance increased significantly in 1998 and remained high, whereas CHL, AZM, and AMP resistance decreased after an initial increase (*5*). Substantial temporal variations in AMR were observed among isolates. AZM resistance increased, whereas SXT susceptibility was retained, possibly owing to shifts in antibiotic treatment patterns. In the 1970s, SXT was the primary treatment for cholera, but AZM and CIP have become the preferred therapy in recent clinical practice (*4*,*13*). Antimicrobial pressure may have contributed to the acquisition of macrolide-resistance genes, including *mphE* and *mphF*. A gradual loss of AMR genes with the wave progression of O139 in other Asian countries may explain the decline of this lineage (*10*). However, our analysis revealed that local O139 strains acquired new AMR genes, particularly those associated with AZM resistance, which enabled continuous transmission in the region.

The study has two primary limitations. First, the analysis was restricted to O139 isolates from a single province from 2013 to 2024, with limited samples. Second, the limited recent global O139 genomic data could have reduced phylogenetic resolution, and these findings may not fully represent the genetic diversity or evolutionary dynamics of O139 strains across broader regions. Despite low pathogenicity, the Anhui O139 strains demonstrated robust colonization and resistance gene transmission, indicating persistent local transmission and the emergence of new resistance patterns.

Conflicts of interest: No conflicts of interest.

Funding: Supported by the National Disease Control and Prevention Administration Public Health Talent Training Program (202303), the Open Fund of the State Key Laboratory of Tea Plant Biology and Utilization (SKLTOF20200131), the Scientific Research Projects of Health Commission of Anhui Province in 2022 (AHWJ2022a022), and the Scientific Research Projects of Health Commission of Anhui Province in 2023 (AHWJ2023A20398).

doi: 10.46234/ccdcw2025.179

[#] Corresponding authors: Jinbao Huang, jinbaohuang@ahau.edu.cn; Zhiguo Cao, caozhiguo@ahcdc.com.cn.

[1] Anhui Provincial Center for Disease Control and Prevention, Hefei City, Anhui Province, China; [2] State Key Laboratory of Tea Plant Biology and Utilization, Anhui Agricultural University, Hefei City, Anhui Province, China; [3] Maanshan City Center for Disease Control and Prevention, Maanshan City, Anhui Province, China; [4] Bozhou City Center for Disease Control and Prevention, Bozhou City, Anhui Province, China; [5] Fuyang City Center for Disease Control and Prevention, Fuyang City, Anhui Province, China; [6] Bengbu City Center for Disease Control and Prevention, Bengbu City, Anhui Province, China.

Submitted: May 11, 2025
Accepted: July 23, 2025
Issued: August 08, 2025

REFERENCES

1. Deen J, Mengel MA, Clemens JD. Epidemiology of cholera. Vaccine

2020;38 Suppl 1:A31-40. http://dx.doi.org/10.1016/j.vaccine.2019.07.078.
2. Ramamurthy T, Garg S, Sharma R, Bhattacharya SK, Nair GB, Shimada T, et al. Emergence of novel strain of *Vibrio cholerae* with epidemic potential in southern and eastern India. Lancet 1993;341(8846):703 – 4. https://doi.org/10.1016/0140-6736(93)90480-5.
3. Cholera Working Group, International Centre for Diarrhoeal Diseases Research, Bangladesh, Albert MJ, Ansaruzzaman M, Bardhan PK, Faruque ASG, Faruque SM. Large epidemic of cholera-like disease in Bangladesh caused by *Vibrio cholerae* O139 synonym Bengal. Lancet 1993;342(8868):387 – 90. https://doi.org/10.1016/0140-6736(93)92811-7.
4. Clemens JD, Nair GB, Ahmed T, Qadri F, Holmgren J. Cholera. Lancet 2017;390(10101):1539 – 49. https://doi.org/10.1016/s0140-6736(17)30559-7.
5. Yu L, Zhou YY, Wang RB, Lou J, Zhang LJ, Li J, et al. Multiple antibiotic resistance of *Vibrio cholerae* serogroup O139 in China from 1993 to 2009. PLoS One 2012;7(6):e38633. https://doi.org/10.1371/journal.pone.0038633.
6. Zhang P, Zhou HJ, Diao BW, Li FJ, Du PC, Li J, et al. A molecular surveillance reveals the prevalence of *Vibrio cholerae* O139 isolates in China from 1993 to 2012. J Clin Microbiol 2014;52(4):1146 – 52. https://doi.org/10.1128/jcm.03354-13.
7. Tao T, Meng XC, Lu MJ, Lin H, Fu GL, Han X. Identification of the first case of Vibrio cholerae O_{139} and its toxin, Anhui Province. J Hyg Res 1998;27(S1):18. https://doi.org/10.19813/j.cnki.weishengyanjiu.1998.s1.007.
8. Dorman MJ, Domman D, Uddin MI, Sharmin S, Afrad MH, Begum YA, et al. High quality reference genomes for toxigenic and non-toxigenic *Vibrio cholerae* serogroup O139. Sci Rep 2019;9(1):5865. https://doi.org/10.1038/s41598-019-41883-x.
9. Wang JZ, Yan MY, Gao H, Lu X, Kan B. *Vibrio cholerae* colonization of soft-shelled turtles. Appl Environ Microbiol 2017;83(14):e00713 – 17. https://doi.org/10.1128/aem.00713-17.
10. Ramamurthy T, Pragasam AK, Taylor-Brown A, Will RC, Vasudevan K, Das B, et al. *Vibrio cholerae* O139 genomes provide a clue to why it may have failed to usher in the eighth cholera pandemic. Nat Commun, 2022;13(1):3864. https://doi.org/10.1038/s41467-022-31391-4.
11. Luo Y, Ye JL, Payne M, Hu DL, Jiang JM, Lan RT. Genomic epidemiology of *Vibrio cholerae* O139, Zhejiang Province, China, 1994-2018. Emerg Infect Dis 2022;28(11):2253 – 60. https://doi.org/10.3201/eid2811.212066.
12. Liang XY, Pei TT, Li H, Zheng HY, Luo H, Cui Y, et al. VgrG-dependent effectors and chaperones modulate the assembly of the type VI secretion system. PLoS Pathog 2021;17(12):e1010116. https://doi.org/10.1371/journal.ppat.1010116.
13. Das B, Verma J, Kumar P, Ghosh A, Ramamurthy T. Antibiotic resistance in *Vibrio cholerae*: understanding the ecology of resistance genes and mechanisms. Vaccine 2020;38 Suppl 1:A83-92. http://dx.doi.org/10.1016/j.vaccine.2019.06.031.

Notes from the Field

An Outbreak of Chikungunya Fever in China — Foshan City, Guangdong Province, China, July 2025

Yihong Li[1]; Siyang Jiang[1]; Meng Zhang[1]; Yan Li[1]; Jianfeng He[1]; Zefeng Yang[2]; Xiqing Huang[2]; Qihua Guan[2]; Zhufeng Li[3]; Jiamin Xie[3]; Qun Lin[4]; Hong Li[5]; Wingsum Li[6]; Yuenshan Lam[6]; Lei Zhou[7]; Min Kang[1,#]

Chikungunya fever (CF) is caused by chikungunya virus (CHIKV), which is transmitted to humans through the bites of infected female *Aedes* mosquitoes. CHIKV has been documented in over 110 countries across Asia, Africa, Europe, and the Americas (*1*). China reported its first imported case of CF in 2008. Between 2010 and 2019, local outbreaks resulting from imported cases were documented in Guangdong (*2*), Zhejiang (*3*), and Yunnan provinces (*4*).

On July 9, 2025, Foshan City, Guangdong Province reported a cluster of CF cases. As of July 26, a total of 4,824 confirmed cases had been reported (*5*) across 12 prefecture-level cities in Guangdong, with 4,754 cases (98.5%) occurring in Foshan and 70 cases (1.5%) distributed among the other 11 prefectures. The majority of cases were concentrated in Shunde District of Foshan, which accounted for 4,208 cases (87.2% of all provincial cases).

Among the confirmed cases, the earliest symptom onset date was June 16. Daily case reports reached their peak on July 19, with 681 cases recorded. The male-to-female ratio was 1:0.97, and the median age was 44 years (range: 0–95 years). Adults aged 15–64 years comprised the largest proportion of cases (3,229 cases; 66.9%), followed by older adults aged ≥65 years (940 cases; 19.5%), school-aged children aged 5–14 years (546 cases; 11.3%), and young children under 5 years (109 cases; 2.3%).

All cases reported to date were mild, with no severe illness or death documented. A preliminary analysis of the early 1,634 cases in Shunde District revealed that 1,418 cases (86.8%) presented with fever, 1,330 (81.4%) experienced joint pain, 1,070 (65.5%) developed rashes, and 838 cases (51.3%) manifested all three cardinal symptoms.

All cases were confirmed by reverse transcription polymerase chain reaction (RT-PCR) (*6*). Whole genome sequencing (*7*) was performed for 190 cases. Genomic sequence analysis demonstrated high homology among these viral strains, which all belonged to the Central African Clade of the East-Central-South African (ECSA) genotype.

Following the outbreak, authorities implemented comprehensive surveillance and case management protocols. Active case detection was combined with differential screening to distinguish dengue from CF among patients presenting with fever, rash, or joint pain. Healthcare facilities in Foshan began conducting nucleic acid testing for CHIKV as part of routine diagnostic procedures.

Confirmed cases received targeted vector control interventions within seven days of symptom onset. These measures included installing insecticide-treated window screens and bed nets at patients' rooms, along with applying residual repellents to living spaces. This patient-focused strategy provided continuous mosquito protection during the infectious period, effectively interrupting virus transmission from humans to vectors.

Simultaneously, comprehensive vector control measures were implemented across affected communities. Targeted adulticide spraying and systematic elimination of mosquito breeding sites were conducted within a minimum 100-meter radius of confirmed case residences, workplaces, and frequently visited locations. Real-time vector surveillance using the Breteau Index and Area Density Index provided critical metrics to assess and optimize transmission control effectiveness.

doi: 10.46234/ccdcw2025.172

[#] Corresponding author: Min Kang, kangmin@cdcp.org.cn.

[1] Guangdong Provincial Center for Disease Control and Prevention, Guangzhou City, Guangdong Province, China; [2] Foshan Center for Disease Control and Prevention, Foshan City, Guangdong Province, China; [3] Shunde District Center for Disease Control and Prevention, Foshan City, Guangdong Province, China; [4] Lecong Hospital of Shunde, Foshan City, Guangdong Province, China; [5] The Eighth Affiliated Hospital, Southern Medical University (The First People's Hospital of Shunde, Foshan), Foshan City, Guangdong Province, China; [6] Centre for Health Protection, Department of Health, Hong Kong Special Administrative Region, China; [7] Chinese Center for Disease Control and Prevention, Beijing, China.

Submitted: August 02, 2025
Accepted: August 03, 2025
Issued: August 03, 2025

REFERENCES

1. World Health Organization. Chikungunya fact sheet. Geneva: World Health Organization; 2025. https://www.who.int/news-room/fact-sheets/detail/chikungunya. [2025-8-1].
2. Wu D, Wu J, Zhang Q, Zhong H, Ke C, Deng X, et al. Chikungunya outbreak in Guangdong Province, China, 2010. Emerg Infect Dis. 2012;18(3):493 – 5. https://doi.org/10.3201/eid1803.110034.
3. Pan J, Fang C, Yan J, Yan H, Zhan B, Sun Y, et al. Chikungunya Fever Outbreak, Zhejiang Province, China, 2017. Emerg Infect Dis. 2019;25(8):1589 – 91. https://doi.org/10.3201/eid2508.
4. Liu LB, Li M, Gao N, Shen JY, Sheng ZY, Fan DY, et al. Epidemiological and clinical characteristics of the chikungunya outbreak in Ruili City, Yunnan Province, China. J Med Virol. 2022;94(2):499 – 506. https://doi.org/10.1002/jmv.27302.
5. Guangdong Provincial Center for Disease Control and Prevention. Chikungunya Surveillance Data in Guangdong Province (July 20–26, 2025). 2025. https://cdcp.gd.gov.cn/ywdt/tfggwssj/content/post_4750007.html. [2025-8-1]. (In Chinese).
6. National Health Commission of the People's Republic of China. WS/T 590-2018 Diagnostic Criteria for Chikungunya Fever. 2018. https://www.ndcpa.gov.cn/jbkzzx/crb/common/content/content_1656311979820519424.html. [2025-8-1]. (In Chinese).
7. Quick J, Grubaugh ND, Pullan ST, Claro IM, Smith AD, Gangavarapu K, et al. Multiplex PCR method for MinION and Illumina sequencing of Zika and other virus genomes directly from clinical samples. Nat Protoc. 2017;12(6):1261 – 76. https://doi.org/10.1038/nprot.2017.066.

Youth Editorial Board

Indexed by Science Citation Index Expanded (SCIE), Social Sciences Citation Index (SSCI), PubMed Central (PMC), Scopus, Chinese Scientific and Technical Papers and Citations, and Chinese Science Citation Database (CSCD)

The inauguration of *China CDC Weekly* is in part supported by Project for Enhancing International Impact of China STM Journals Category D (PIIJ2-D-04-(2018)) of China Association for Science and Technology (CAST).

CCDC weekly

Vol. 7 No. 32 Aug. 8, 2025

Responsible Authority
National Disease Control and Prevention Administration

Sponsor
Chinese Center for Disease Control and Prevention

Editing and Publishing
China CDC Weekly Editorial Office
No.155 Changbai Road, Changping District, Beijing, China
Tel: 86-10-63150501, 63150701
Email: weekly@chinacdc.cn

CSSN
ISSN 2096-7071 (Print)
ISSN 2096-3101 (Online)
CN 10-1629/R1